Development and use of photoelasticity laboratory for Montana State College.
by Max A Burroughs

A THESIS Submitted to the Graduate Faculty in partial fulfillment of the requirements for the degree of Master of Science in Civil Engineering at Montana State College
Montana State University
© Copyright by Max A Burroughs (1950)

Abstract:
The photoelastic approach to model study is presented for an indeterminate structure. The appendix to the thesis briefly contains the theory of light, stress, and photoelasticity that is involved in the solution of the problem.

The design and construction of the apparatus is presented as well as the visual and quantitative distribution of stresses acting at a section. The photoelastic stress results are compared with an analytical solution.

A haunched-girder bant model was used in the investigation.' The results obtained by the two methods mentioned were in close agreement at a section away from stress concentration. However, at a point where stress concentration occurs, the photoelastic solution gave a much larger stress than the analytical solution.

THE DEVELOPMENT AND USE OF A PHOTOELASTICITY LABORATORY FOR MONTANA STATE COLLEGE

by

MAX A. BURROUGHS

A THESIS

Submitted to the Graduate Faculty

in

partial fulfillment of the requirements

for the degree of

Master of Science in Civil Engineering

at

Montana State College

Approved:

E. R. Dodge
Head, Major Department

R C DeHart
Chairman, Examining Committee

J. A. Nelson
Dean, Graduate Division

Bozeman, Montana
April, 1950

N378
B944d
Cop2

TABLE OF CONTENTS

	Page
Acknowledgement	3
Abstract	4
Introduction	5
Purpose	5
Importance	5
Previous Work	6
Apparatus Design	7
Behavior of Light	7
Lens and Light Source	8
Mount Design	8
Properties and Preparation of Model	11
Properties	11
Preparation	12
Mounting and Loading Model	17
Photographing the Loaded Model	17
Photoelastic Stress Evaluation of Model	17
The Analytical Solution	39
Conclusion	43
Appendix A, Light Theory as it Pertains to Photoelasticity	47
Appendix B, Stress Relations as They Pertain to Photoelasticity	55
Appendix C, Photoelastic Analysis of Stresses	64

JUL 24 '50

93821

ACKNOWLEDGEMENT

The author takes this opportunity to express appreciation to the following: W. S. Adams for his assistance in the design and construction of the apparatus, Professor J. C. Osborn for all the photographs contained in the thesis, Dr. E. R. Dodge and Professor R. C. DeHart for their suggestions and assistance on the numerous difficulties encountered.

ABSTRACT

The photoelastic approach to model study is presented for an indeterminate structure. The appendix to the thesis briefly contains the theory of light, stress, and photoelasticity that is involved in the solution of the problem.

The design and construction of the apparatus is presented as well as the visual and quantitative distribution of stresses acting at a section. The photoelastic stress results are compared with an analytical solution.

A haunched-girder bent model was used in the investigation. The results obtained by the two methods mentioned were in close agreement at a section away from stress concentration. However, at a point where stress concentration occurs, the photoelastic solution gave a much larger stress than the analytical solution.

INTRODUCTION

Purpose

The purpose of this thesis is to solve a statically indeterminate stress problem by photoelasticity. The experimental results are compared with an analytical solution. Before the photoelasticity solution could be made, it was necessary to design and construct a suitable apparatus.

The development of a permanent accurate apparatus with a substantial saving in money has been attempted.

It is hoped that the photoelastic apparatus will permit engineering students at Montana State College to obtain an introduction to photoelastic analysis. Senior and graduate students may also use the apparatus for specialized study.

Importance

Examples of design problems which are beyond the scope of the analytic methods the designer has at his disposal are numerous. Throughout the airplane structure many members are indeterminate to several degrees, thereby making an exact solution impractical. The mathematical theory of elasticity also becomes highly difficult and tedious when boundaries and loads become irregular. Stress concentrations originate at sharp discontinuities such as fillets, holes, grooves, and small irregularities on the surface. Failure at any point in the structure or machine may ultimately cause complete failure. The true value of the stress concentrations may be of such importance that it must be accurately determined.

The use of photoelasticity makes possible the solution of extremely complicated problems that cannot be reasonably approached by any mathematical solution. Experiments also show that actual stress distribution is not always as computed by the theory of elasticity. This is due to assumptions that must be made concerning the application of external loads and the behavior of internal strain. Therefore, the economical and exact method of photoelasticity may be turned to for a more complete understanding of the internal stress conditions. By photoelastic studies, a visual as well as a quantitative solution can be made.

Previous Work

There have been stress investigations made by photoelasticity for a considerable length of time. Professor E. G. Coker and L. N. Filon of the University of London[1] introduced photoelasticity to the engineering profession. They began their work about 1900.

The solution of problems by photoelasticity has been advanced to the point that many laboratories are supported by grants from various industrial concerns. Refinement of model material has brought forth a resin that yields extremely accurate results. This resin is called Bakelite and its commercial numbering is BT-61-893. Early experiments used models of glass, celluloid, or gelatin.

One of the foremost American engineers today in the photoelasticity

1. Coker, E. G., and Filon, L. N. 1930 TREATISE ON PHOTOELASTICITY, Cambridge Press, London.

field is Dr. Max Mark Frocht[2,3]. The two books by Dr. Frocht provide an excellent background in the field.

APPARATUS DESIGN

The general arrangement of the apparatus is somewhat uniform in all laboratories. An understanding of the apparatus design requires a knowledge of photoelastic theory, and a brief synopsis of the theory will be presented here. Appendix A presents a more thorough explanation.

Behavior of Light

The most simple arrangement is called the plane setup and is shown in Fig. A-5. A light wave coming from a light source is passed through a polaroid lense. The polaroid lense allows only waves vibrating in one plane to continue. This wave next encounters the loaded model. The model material has the property of splitting the wave into two waves, each vibrating parallel to one of the principal stress directions. These two waves next encounter the second polaroid lense and again are converted into a single wave vibrating in one plane.

The plane setup shows the stress lines in the loaded model and also will be used to obtain the isoclinic lines. The purpose of isoclinic lines is explained later.

For an evaluation of the magnitude of the stresses existing in the model, the apparatus requires refinement. The light source is filtered to allow for the passage of waves of one color only, since the length of

---

2. Frocht, M. M. 1941 PHOTOELASTICITY, Vol. 1, John Wiley & Sons, Inc., New York.
3. Frocht, M. M. 1946 PHOTOELASTICITY, Vol. 2, John Wiley & Sons, Inc., New York.

the light wave is used in the stress-optic relationship. In addition, a quarter-wave plate is placed on each side of the stressed model. The quarter-wave plates retard the wave after it has passed through the polaroid lens by $\frac{1}{4}$ wave. (See Fig. A-4) Such light is referred to as circularly polarized. The stress pattern only is shown by a circularly polarized setup.

With the two setups mentioned, a visual and quantitative solution can be made.

Lens and Light Source

A light source manufactured for photoelastic purposes was purchased at a cost of $450 [4]. This source (see Fig. 1) consists of a mercury light illuminator, filter for 5461 Å, condensing lens, and collimating lens. The light emitted is green and is parallel to the longitudinal axis of the lenses. The diameter of the light field is $8\frac{1}{2}$ inches. Polaroid and quarter-wave plates were also purchased at a total cost of $34. These four plates were also $8\frac{1}{2}$ inches in diameter.

Mount Design

The design and construction of a suitable mount for the purchased equipment was necessary. The commercial metal mount costs approximately $450. It was decided a wooden mount could be substituted without any great loss in accuracy. The total cost of the wooden mount was $20. Fig. 2 gives the necessary data for the mount construction. Select grade oak was used throughout, with the exception of the lens frames and they

4. THE POLARIZING INSTRUMENT COMPANY, 630 Fifth Avenue, New York

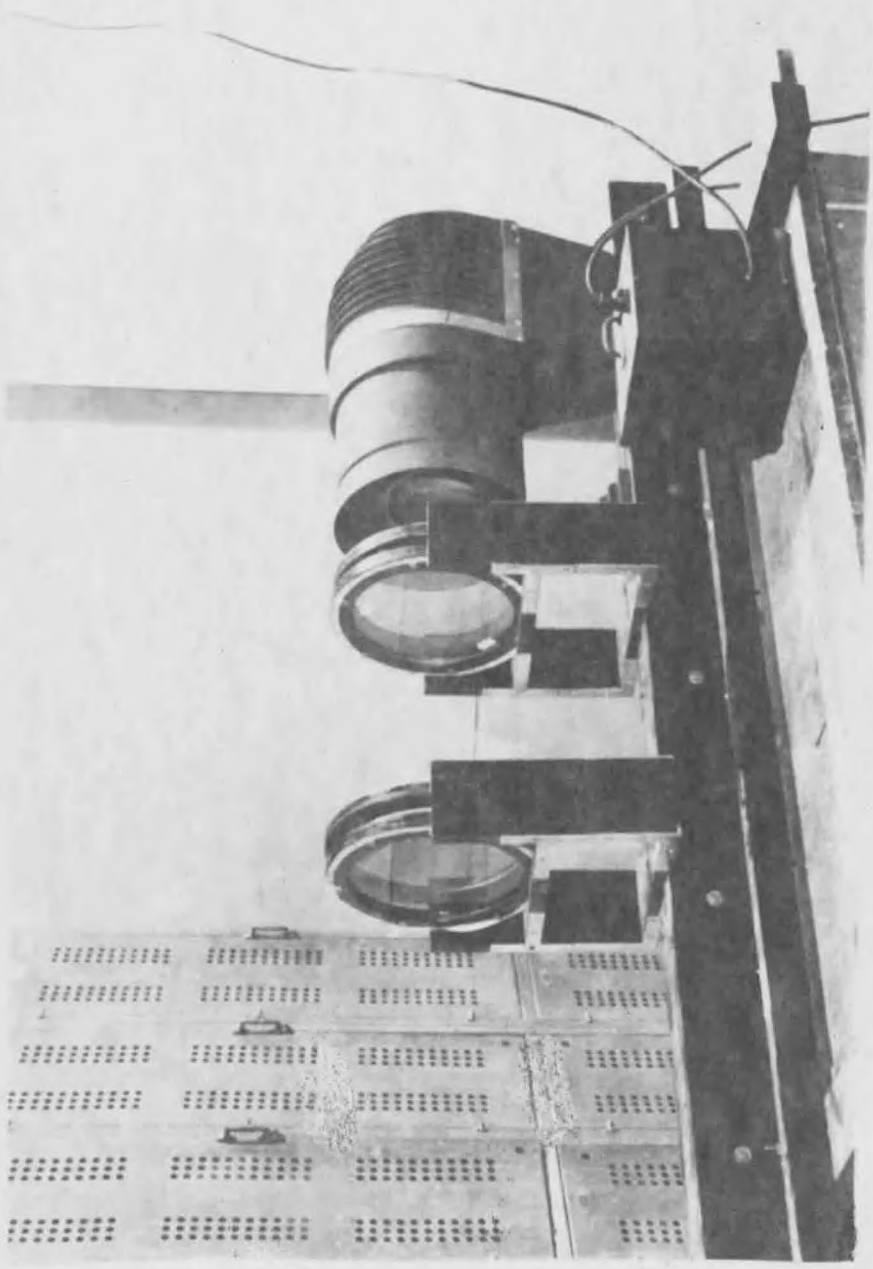
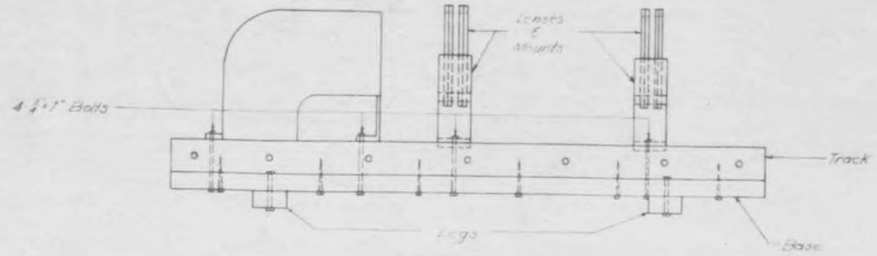


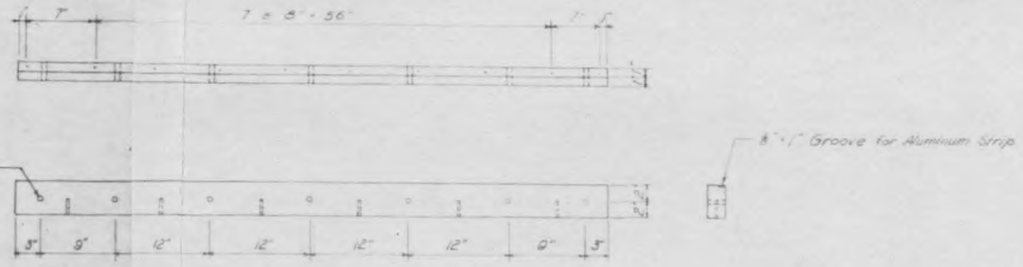
Fig. 1 Assembled Photoelastic Apparatus



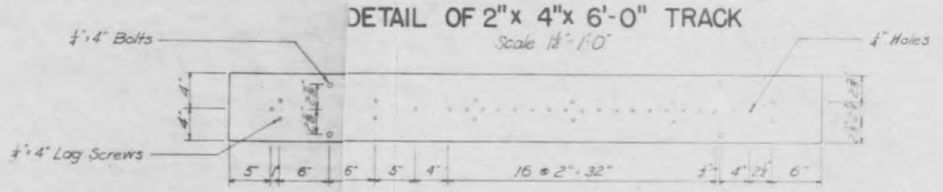
UNMOUNTED PLAN VIEW



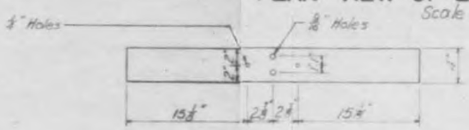
MOUNTED ELEVATION VIEW
Scale 1½"=1'0"



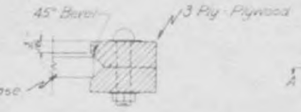
DETAIL OF 2"x 4"x 6'-0" TRACK
Scale 1½"=1'0"



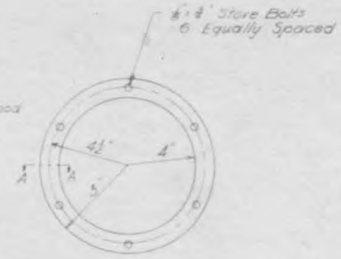
PLAN VIEW OF 2"x 8"x 6'-0" BASE
Scale 1½"=3'0"



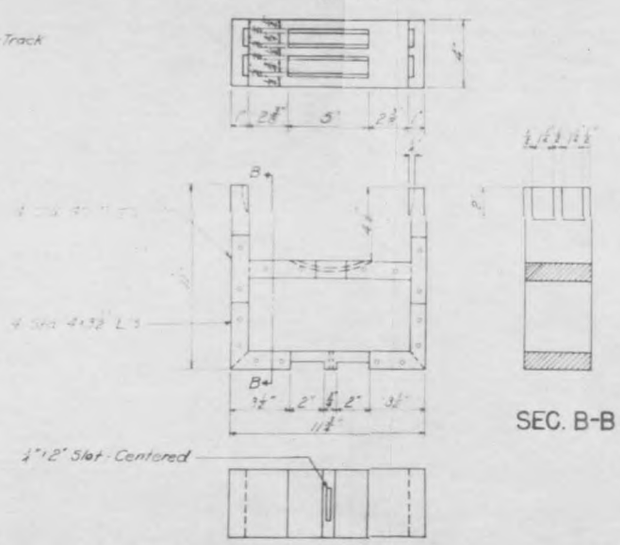
PLAN VIEW OF 2"x 4"x 3'-0" LEGS
Scale 1½"=1'0"



SEC. A-A
Scale 1"=1"

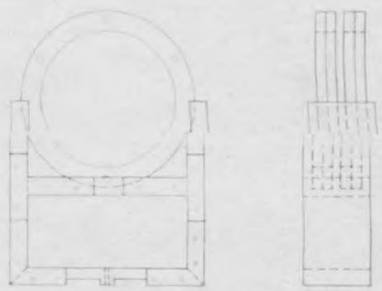


DETAIL OF LENSE FRAME
Scale 3"=1'0"



DETAIL OF LENSE MOUNT
Scale 3"=1'0"

SEC. B-B



ASSEMBLED LENSES & MOUNTS
Scale 3"=1'0"

Note: Paint All Wood With Black Enamel

BILL OF MATERIALS

Type	Quantity
Lumber - Oak except plywood	
2"x4"	18 ft
2"x8"	6 ft
1"x4"	8 ft
¾" Plywood - 2 ft. square	4 sq. ft
Hardware	
⅜"x¾" Store Bolts	24
⅝"x7" Bolts	4
⅝"x5" Bolts	7
½"x4" Bolts	4
¼"x4" Lag Screws	12
Iron Tee Plates - Std. 4"x4"	8
Iron Corner Plates - Std. 4"x3"	8
Aluminum Strip - ⅜"x1"	6 ft
Black Enamel	1 qt.

DESIGN FOR
PHOTOELASTICITY LABORATORY
DESIGNED BY W.S. ADAMS & M.A. BURROUGHS
DRAWN BY M.A. BURROUGHS
DATE JUNE 1949 MONTANA STATE COLLEGE

Fig. 2

were built from 3/8 inch plywood. Fig. 1 is a photograph of the completed apparatus.

PROPERTIES AND PREPARATION OF MODEL

Photoelasticity resin, commonly called Bakelite, was used for the model. Three sheets, approximately 6 in. x 11 in. x $\frac{1}{4}$ in., were obtained for $14.50 per sheet. The commercial numbering of the resin is BT-61-893[5].

Properties

According to Frocht[6], the following properties are necessary for an ideal photoelastic material:

(a) The material must be transparent.

(b) It must be easily machinable to prevent excess building costs.

(c) The optical sensitivity must be high so stress lines may be counted easily.

(d) It must have the proper hardness -- not too brittle to cause machining difficulties but of sufficient hardness so that clamping during machining or other operations will not cause distortion or permanent stresses.

(e) There must be an absence of undue optical or mechanical creep.

(f) There must be freedom of initial stresses.

(g) The material must be isotropic.

---

5. Ibid.
6. Frocht, M. M. 1941 op. cit., p. 323.

(h) Linear stress-strain and linear stress-fringe relations must exist.

(i) The material must have a high enough modulus of elasticity so that the models suffer small deformations only and the shape stays essentially constant.

(j) There must be a constancy of properties during moderate changes in temperature and treatment.

(k) The cost of the material must be moderate.

Bakelite is one of the most ideal materials with which to work at present. Frocht[7] presents the following physical properties of Bakelite: Its linear-stress relation holds till 6000 psi., and its stress-fringe relation holds to 7000 psi. The modulus of elasticity is about 615,000 psi. The tensile strength is 17,000 psi. for a five minute loading. Poisson's ratio is 0.365.

Preparation

Frocht[8] gives the following chronological rules for building a model:

(a) Trim the sealed or cast edges of the plate and anneal if necessary. This necessity will be revealed by inspection in the polariscope.

(b) Store the annealed material for several months or years before using. Time seems to relieve some of the initial stresses.

---

7. Ibid., p. 326.
8. Ibid., p. 360.

(c) Cut a piece of material, a blank, slightly larger than that necessary for the overall dimensions of the model.

(d) Turn or mill the face of this blank to within 0.020 in. of the desired thickness.

(e) Examine this blank in the polariscope, using oil to increase the transparency. Additional annealing, if required by the material, should be done at this stage.

(f) Grind the blank to the desired thickness.

(g) Rough Polish with felt cloth and jewelers rouge.

(h) Lay out the shape of the model on the roughly polished blank.

(i) Cut with a scroll or saw to 1/16 in. of the true dimensions, and machine with an end mill or file to within 0.030 in. of the shape.

(j) Give the model its final polish with a washed and rinsed Selvyt Cloth.

(k) Carefully machine the polished model to its final dimensions.

(l) Make investigation or take loaded model pictures immediately after step k is completed.

The Bakelite sheet in its original shape was put between the crossed polaroid lenses to determine the condition of initial stress. There were severe edge stress conditions extending about $\frac{1}{4}$ in. into the plate. These original stresses were apparently set up when the sheet was molded.

The edge stresses were removed by trimming the $\frac{1}{4}$ in. off with a coping saw. This operation did not set up any permanent stresses as the temperature of the material was not changed a large amount.

The faint stress lines existing in the plate proper were removed by annealing. This process consisted of placing the material on a solid smooth glass surface and placing it within an oven. By slowly changing the heat from 0 to 250 and back to 0 degrees, the internal stresses were removed. The process took four cycles to remove all the internal stresses, each cycle requiring about 12 hours.

As suggested by Frocht, nonuniformity in thickness would disperse light and cause a blurred stress pattern. The sheets were not of uniform thickness and were ground to a thickness ±0.020 in.[9]. Unless a laboratory has a machine reserved for plastic work only, it is very difficult to approach the required limitation by milling.

For this experiment a surface grinder was used to obtain the required uniform thickness. The final thickness varied ±0.005 in. The only grinder available held all stock in place by a magnetic field. The nonmagnetic Bakelite sheet required some additional attachments to hold it.

Metal clips were shaped to fit the ends of the plate and contact the magnetic field. It was, however, impossible to develop sufficient contact area due to the limited size of the magnetic table and this method was abandoned.

---

9. Ibid., p. 361.

The next and most successful attempt resulted in gluing the Bakelite to a cast iron block. Lepage's glue was used. It was quite difficult to obtain enough bond between the cast iron and the Bakelite with the glue. This step in the model construction should be investigated further.

The sheet was hand polished until all scratches produced by the surface grinder were removed. Emery cloth of grades 240, 320, and 600 gave a final surface clear of all but the very minute marks. Crocus cloth of grade NHB was first tried but it was not hard enough to remove the scratches. Garnet paper, wet or dry, of grades 2/0 and 4/0 did not successfully remove the marks as it too was not hard enough.

The model was cut out of the sheet $\frac{1}{4}$ in. larger than true size. The oversize dimension was precaution against chipping or other injury to the model. See Fig. 4 for the finished model.

From the rough model the exact size was achieved by hand filing. The filing operation took considerable time but the finished model had edges nearly perpendicular to the faces and a stress-free condition.

Final polishing of the model by Selvyt cloth and jewelers rouge was attempted by hand without satisfactory results. The success of this step calls for a firm polishing wheel. This operation, when completed, eliminates all scratches.

The model (Fig. 4) had pin end conditions. The diameters of the holes for the pins were 0.1875 in. The final diameter was obtained by starting with a 1/16 in. drilled hole and increasing it by 1/32 in. increments. This gradual enlargement of the hole was precaution against chipping.

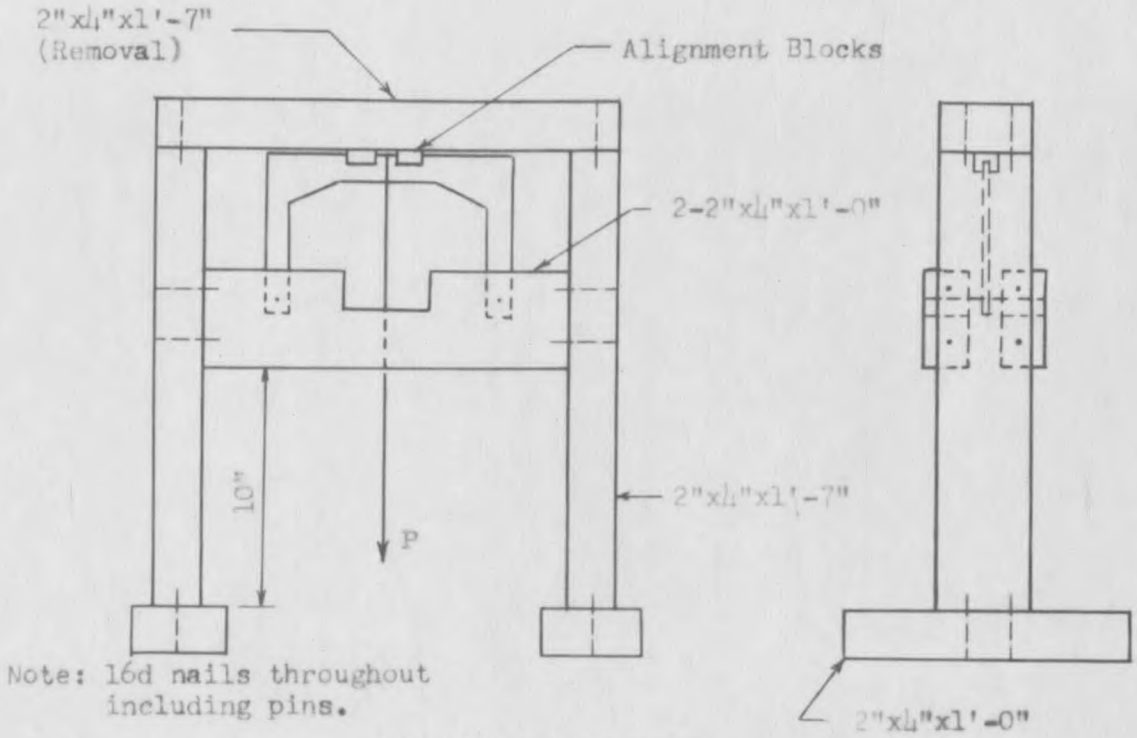


Fig. 3 Loading Frame
Scale: $1\frac{1}{2}$"=1'-0"

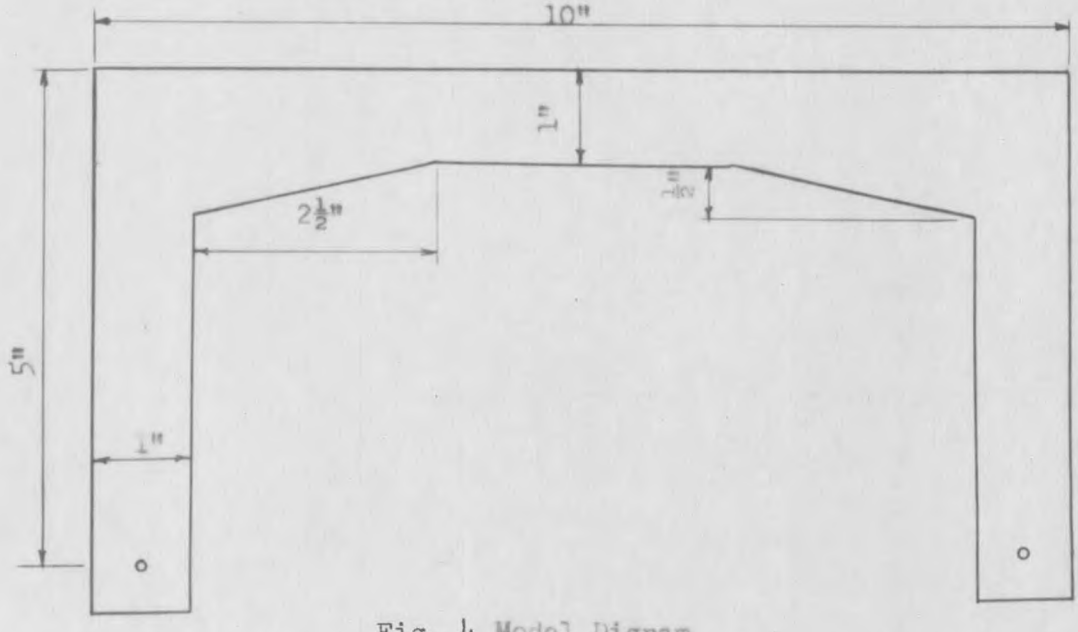


Fig. 4 Model Digram
Scale: $\frac{1}{2}$"=1"

The pins used were 6d nails. A wire and turnbuckle was attached to the columns at each pin to prevent horizontal movement that might result from imperfection in the pin-hole fitting.

Mounting and Loading the Model

A loading frame was constructed for the model as shown in Fig. 3. The frame was built sufficiently rigid to prevent appreciable deflection.

The load consisting of a weighted bucket was applied at the centerline of the model by a wire loop. The total weight applied to the model was 58 lb. This weight gave a clear stress pattern and did not pass the allowable stress-fringe relationship.

Photographing the Loaded Model

A 2¼ by 3¼ in. Eastman Recomar camera was used in taking the pictures. (Figs. 5-15). Super XX Kodak film with an exposure time of 1½ minutes and an f-16 opening gave good results. The only light coming into the camera was that passing the second polaroid lens.

It is not necessary to go to the expense of making photographs. A 5 by 7 in. camera may be set up and the image on the frosted glass traced. This method is as accurate as the one used in this paper. A large saving in time would also result in the tracing process.

PHOTOELASTIC STRESS EVALUATION OF MODEL

For a more complete development of the theory and explanation of photoelastic analysis, the reader is referred to Appendix A, B, and C or references 2 and 3. The following presents only the method of analysis used.

The photoelastic method of stress analysis is based upon the discovery that in a model of uniform thickness the fringe order is constant at all points at which the difference between principal stresses is constant[10].

This law can be expressed by the equation:

$$n = ct(p-q) \qquad (1)$$

where n = fringe order
c = constant of material and light
t = model thickness
(p-q) = difference in principal stresses

The fringe order at any point can be determined from the stress pattern. (Fig. 5). The dark lines are fringes, each of which is a locus of points at which the difference in principal stresses is constant. Fig. 5 shows the model under a concentrated center load of 58 lb. The fringe order is determined by counting the number of stress lines or fringes that move through a given point as the load is gradually applied. In Fig. 5, five stress lines may be counted at the column-girder intersection while actually seven lines moved through this point during application of the load. The sources or points at which the stress lines first begin to form are also best determined by observation.

The constant, c, which depends on the model material and light used, is determined by calibration as shown later.

The term (p-q) is the difference between the principal stresses. This is the term that is to be evaluated, as all other parts of the equation will be known.

---

10. Riggs, Norman C. and Frocht, Max M. 1938 STRENGTH OF MATERIALS, The Ronald Press Company, New York, p. 375.

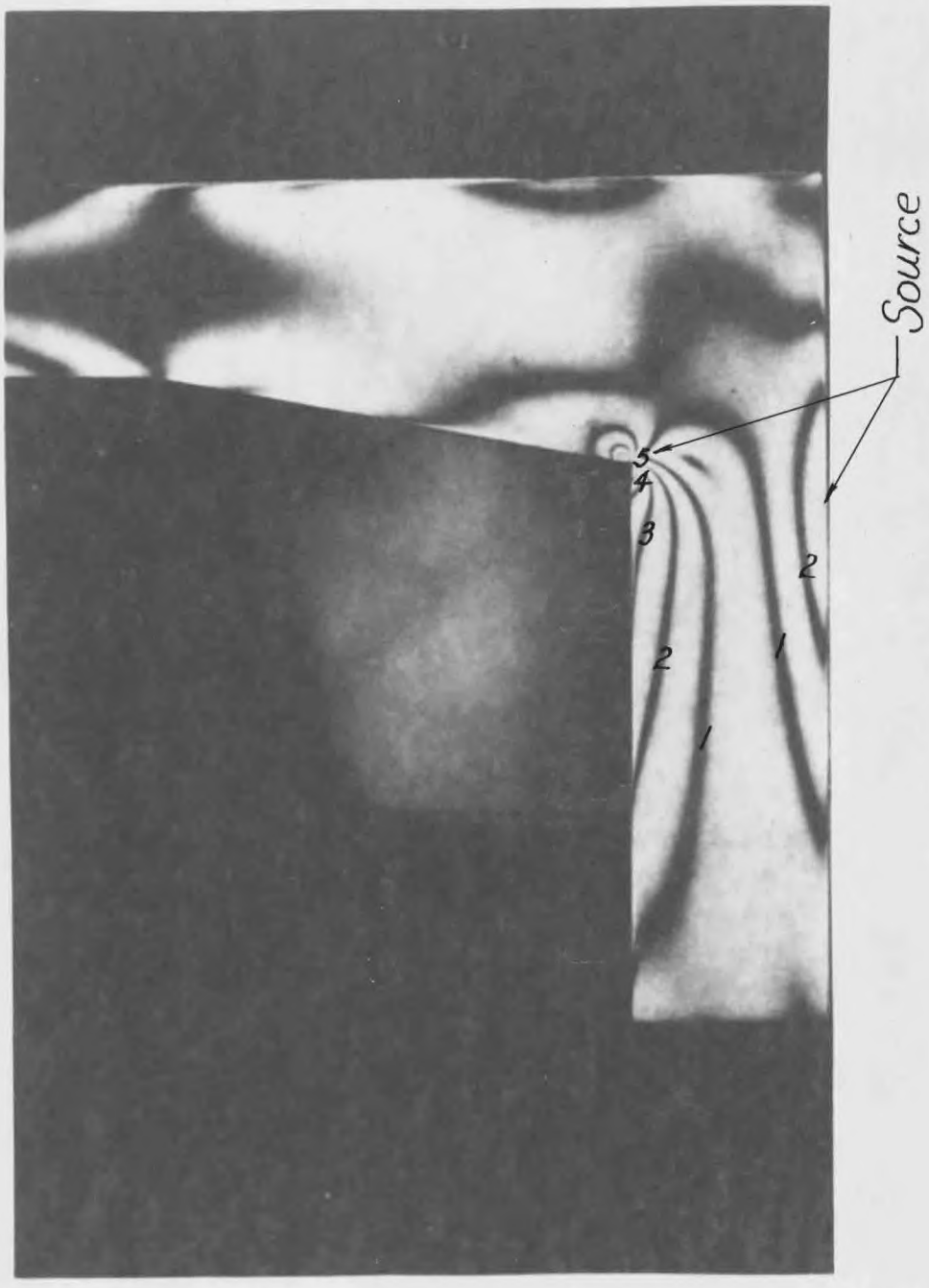


Fig. 5 Stress Pattern (Circularly Polarized Setup)

The next problem is to separate and evaluate p and q for the point or section under investigation. But before this step can be completed, the magnitude and direction of the shearing stress at the point or section in question must be known. (See Appendix C).

It can be shown that (see Appendix B),

$$Sxy = \frac{p-q}{2} \sin 2\phi \qquad (2)$$

where Sxy is the shearing stress existing on a plane parallel to the horizontal axis and ϕ is the angle between the x axis and the maximum positive principal stress. (See Appendix B). It must be remembered that no shearing stresses exist on the planes containing principal stresses. (See Fig. 16). The angle ϕ at any point is determined from the isoclinic lines shown in Figs. 6-15. For convenience, a composite plot of the ten isoclinics is shown in Fig. 17. An isoclinic is a locus of points at which there is equal inclination of principal stresses. A 10 degree isoclinic denotes that one principal stress has its line of action inclined 10 degrees from the x axis. It is now possible to compute the horizontal shearing stress at any point in the model. Fig. 18 shows the variation in ϕ and p-q values.

The direction of the shear stress can be determined by the following rule[11]. Fig. 16 shows an element with the principal stresses acting on the sides and the shear stress acting on the horizontal plane which is under investigation. The direction of the angle between a normal drawn to the shear plane and the extended line of action of the algebraically

11. Frocht, M. M. 1941 op cit., p. 252.

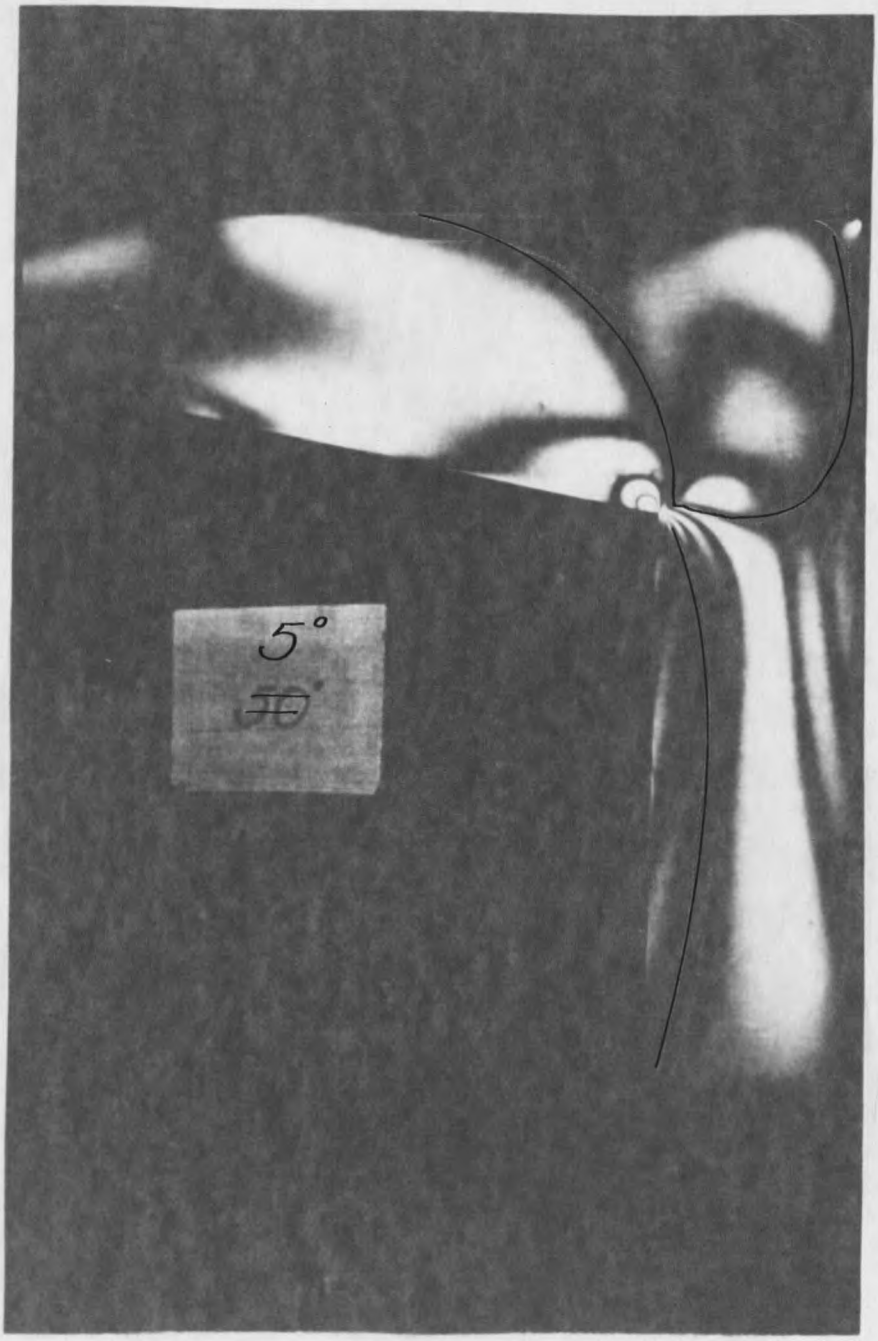


Fig. 6 5° Isoclinic Lines (Plane Setup)

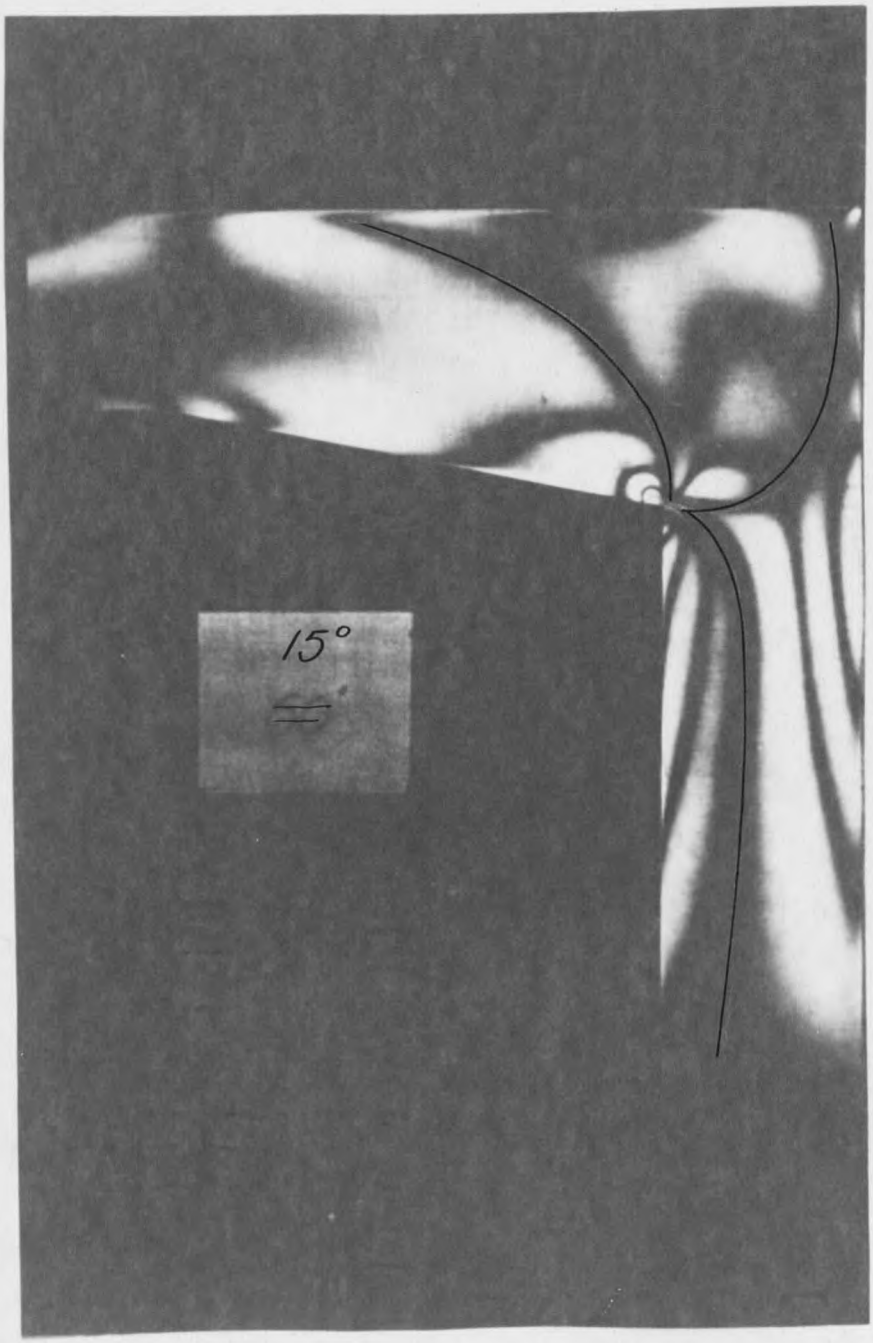


Fig. 7 15° Isoclinic Lines (Plane Setup)

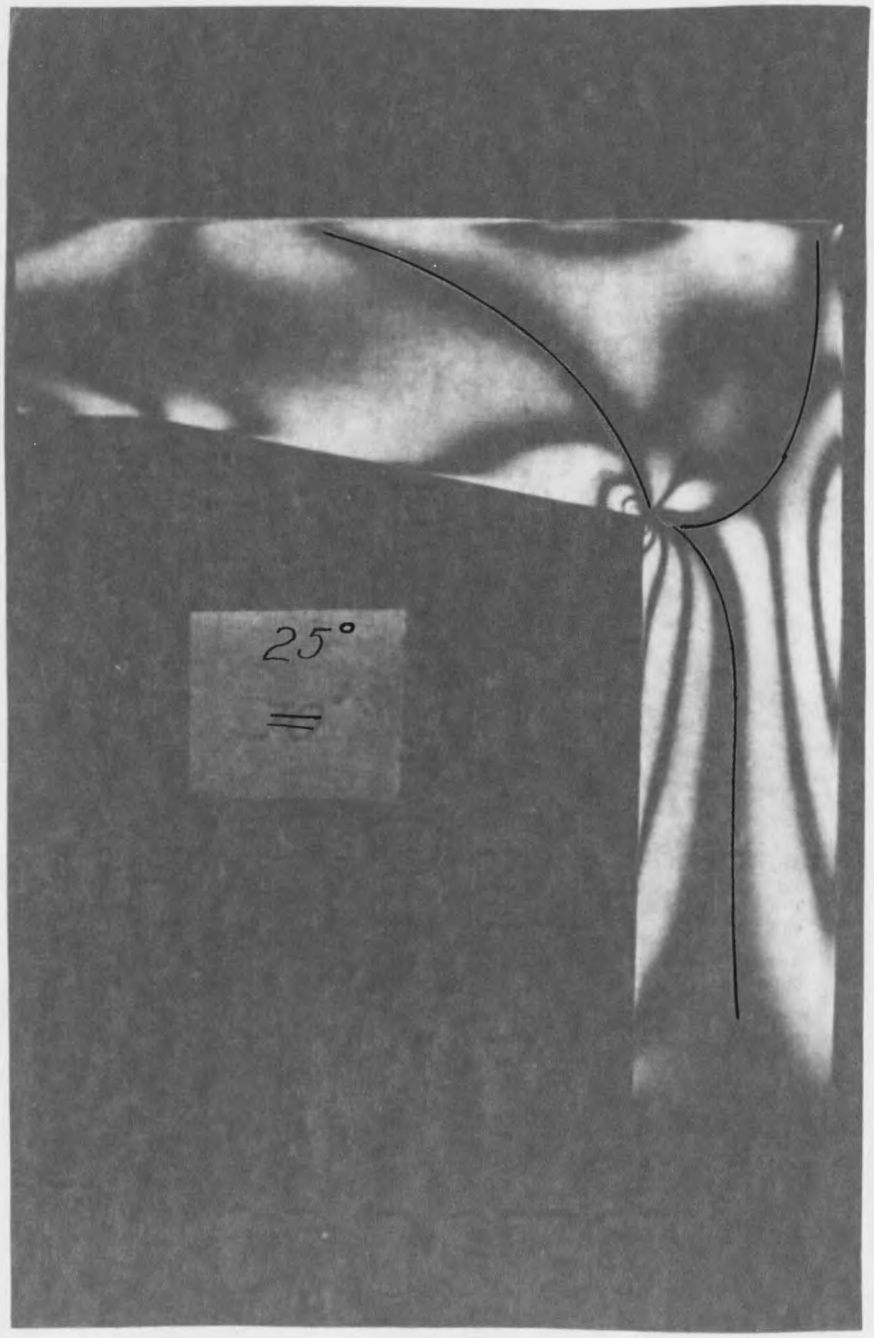


Fig. 8 25° Isoclinic Lines (Plane Setup)

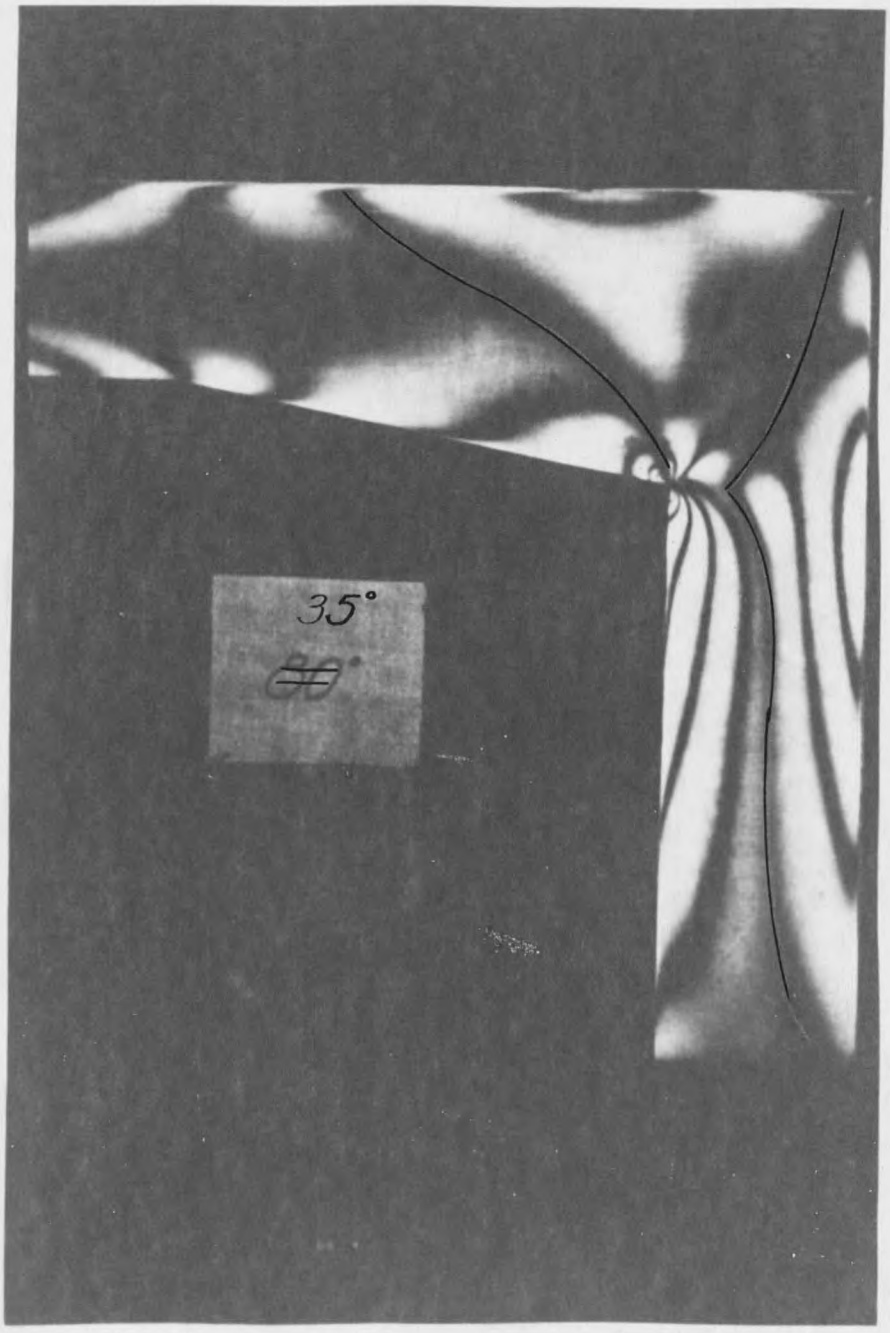


Fig. 9 35° Isoclinic Lines (Plane Setup)

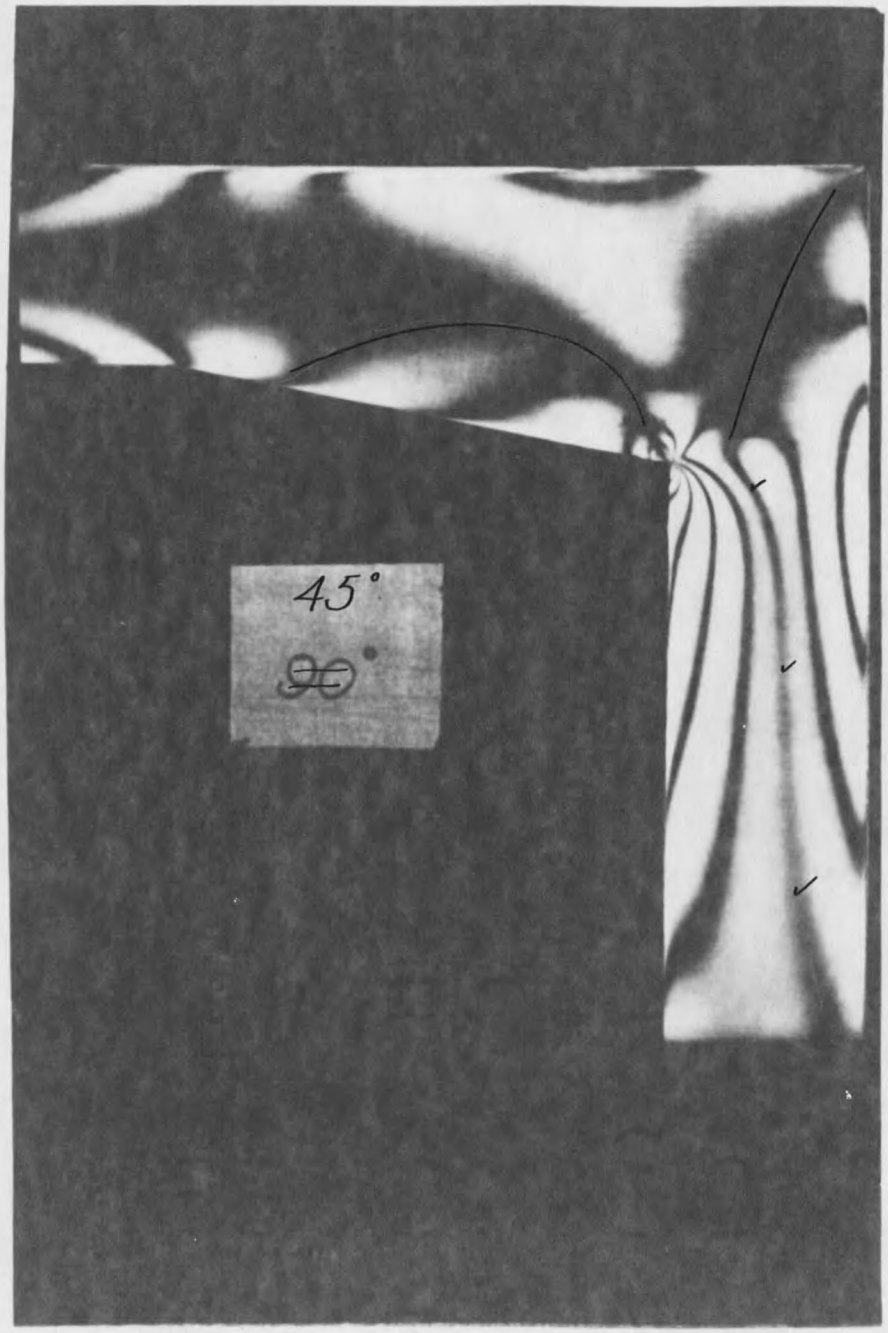


Fig. 10 45° Isoclinic Lines (Plane Setup)

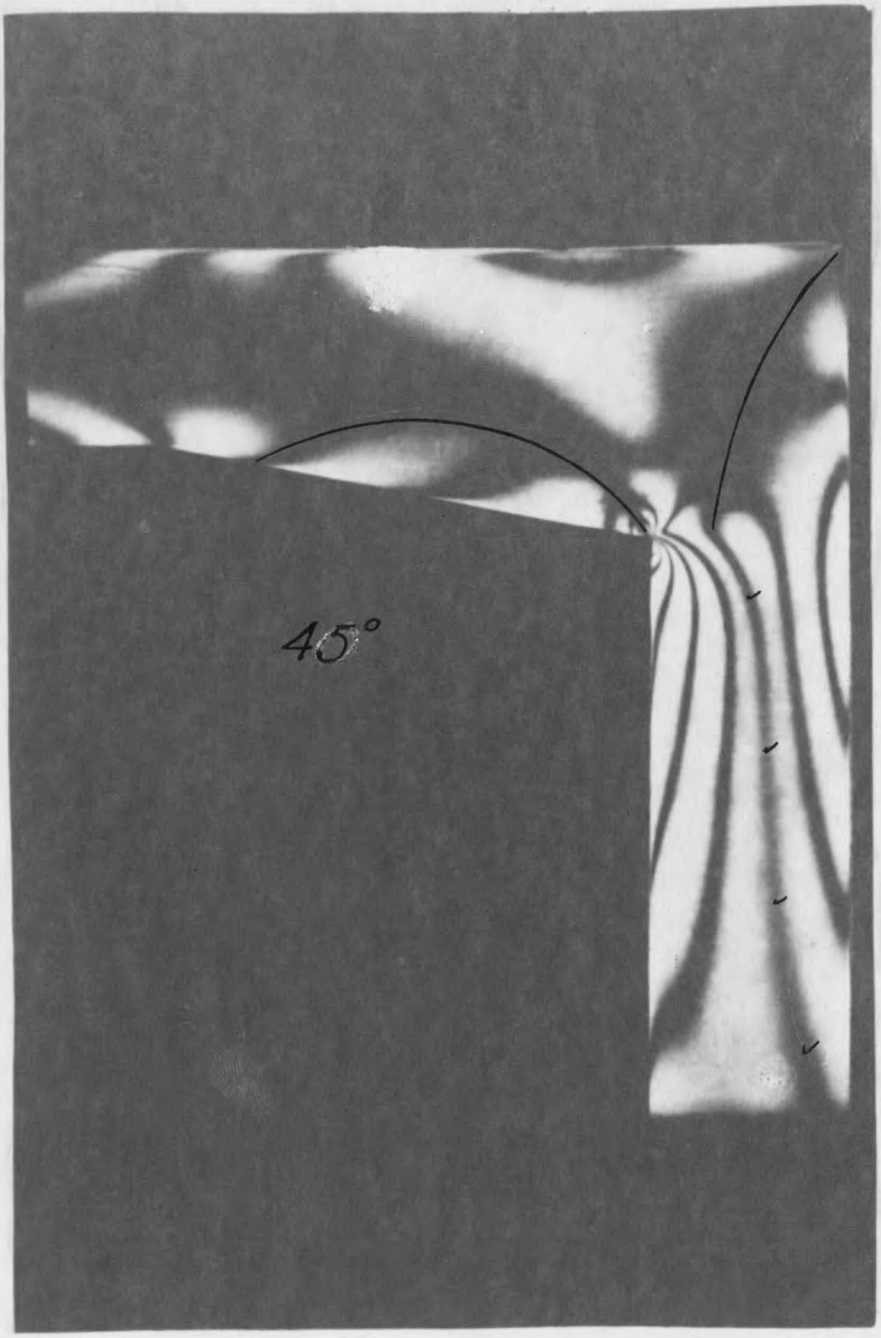


Fig. 11 45° Isoclinic Lines (Plane Setup)

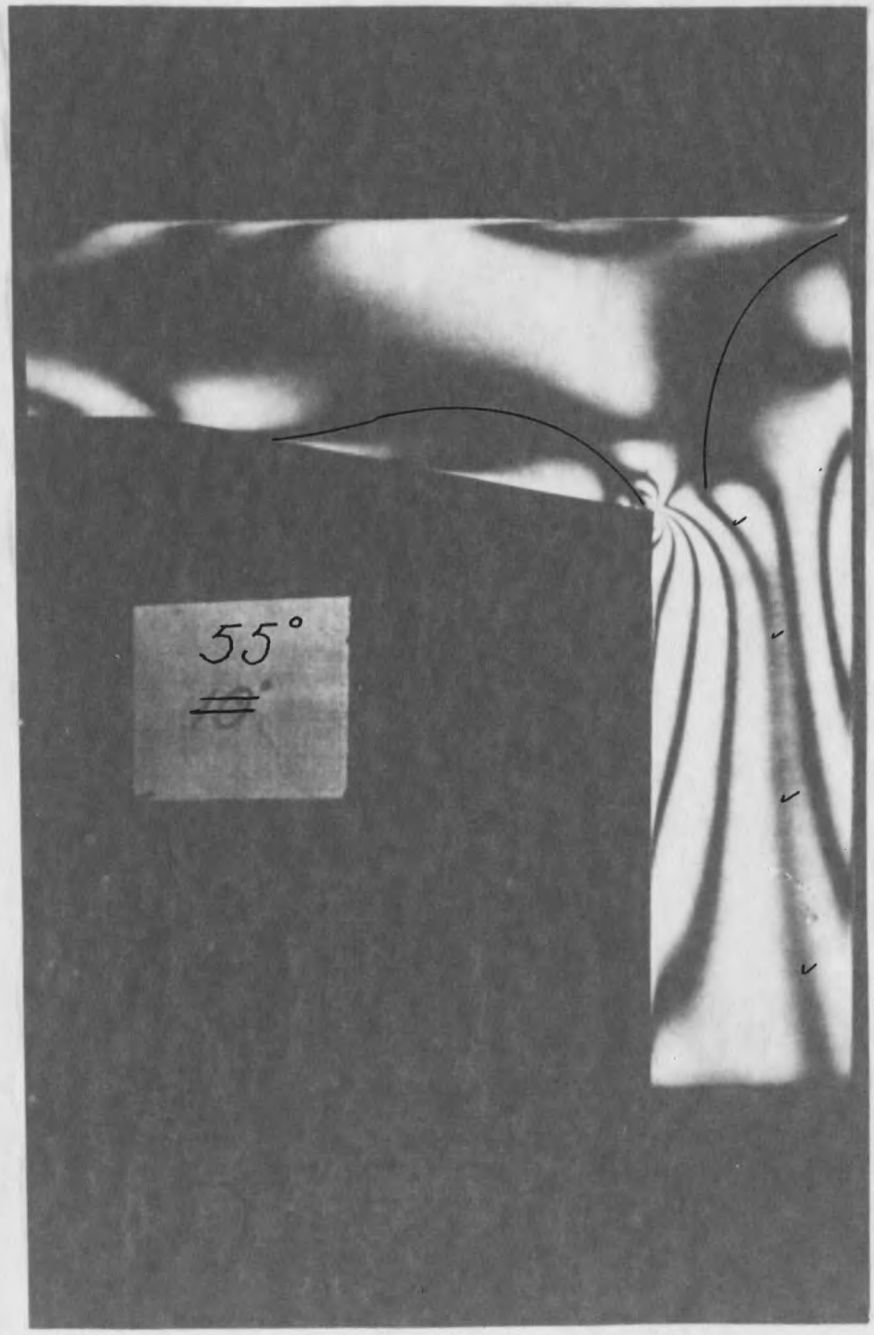


Fig. 12 55° Isoclinic Lines (Plane Setup)

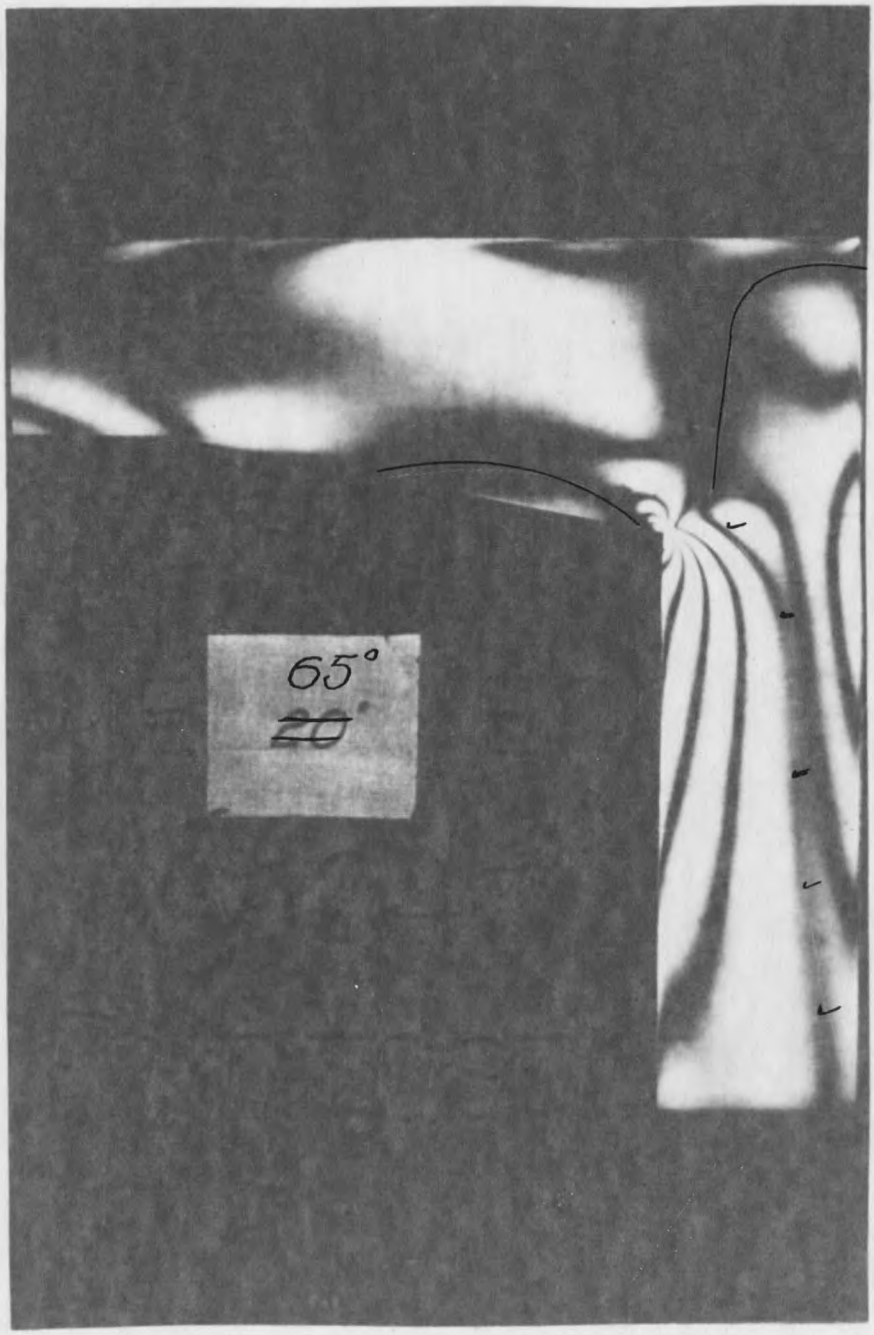


Fig. 13 65° Isoclinic Lines (Plane Setup)

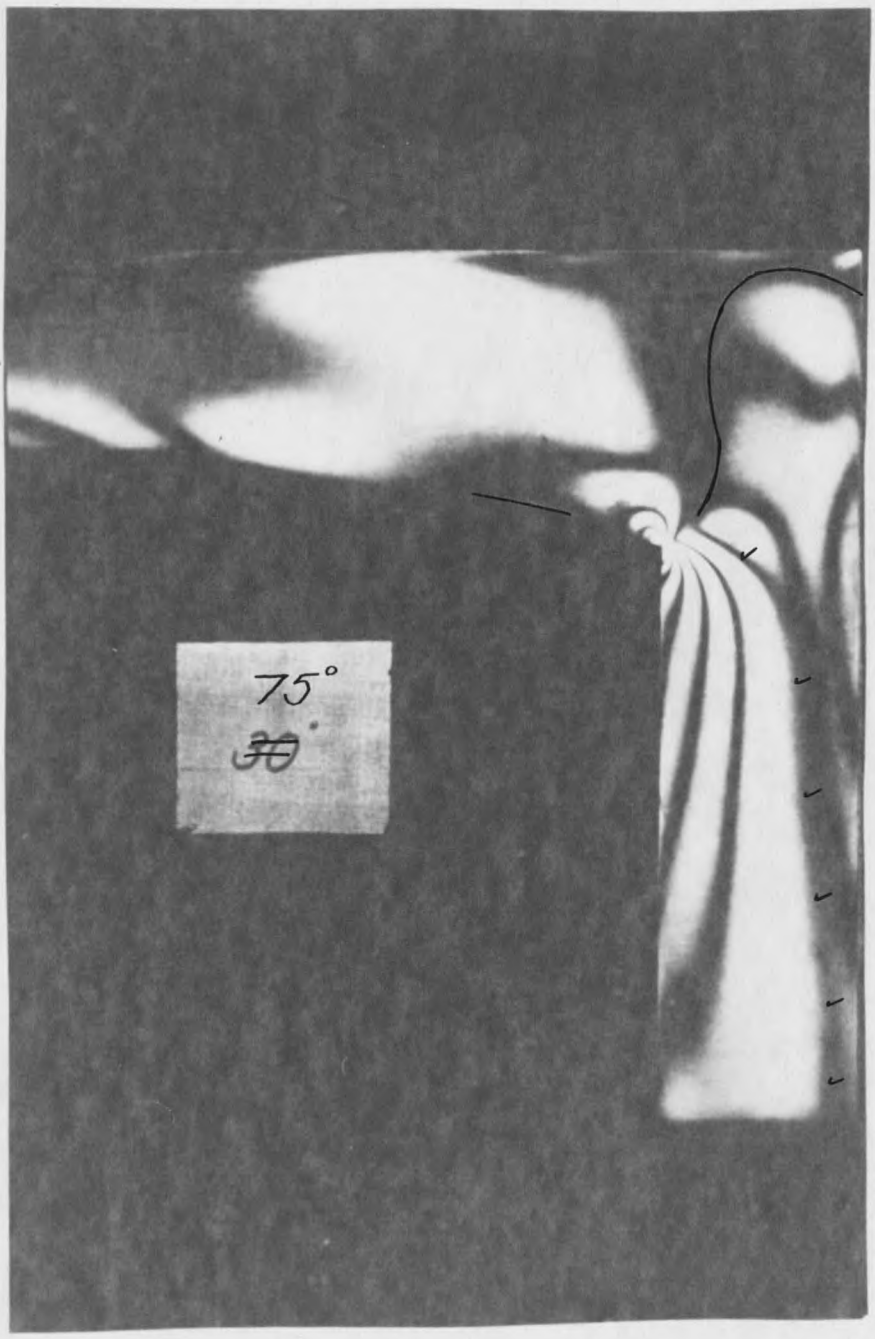


Fig. 14 75° Isoclinic Lines (Plane Setup)

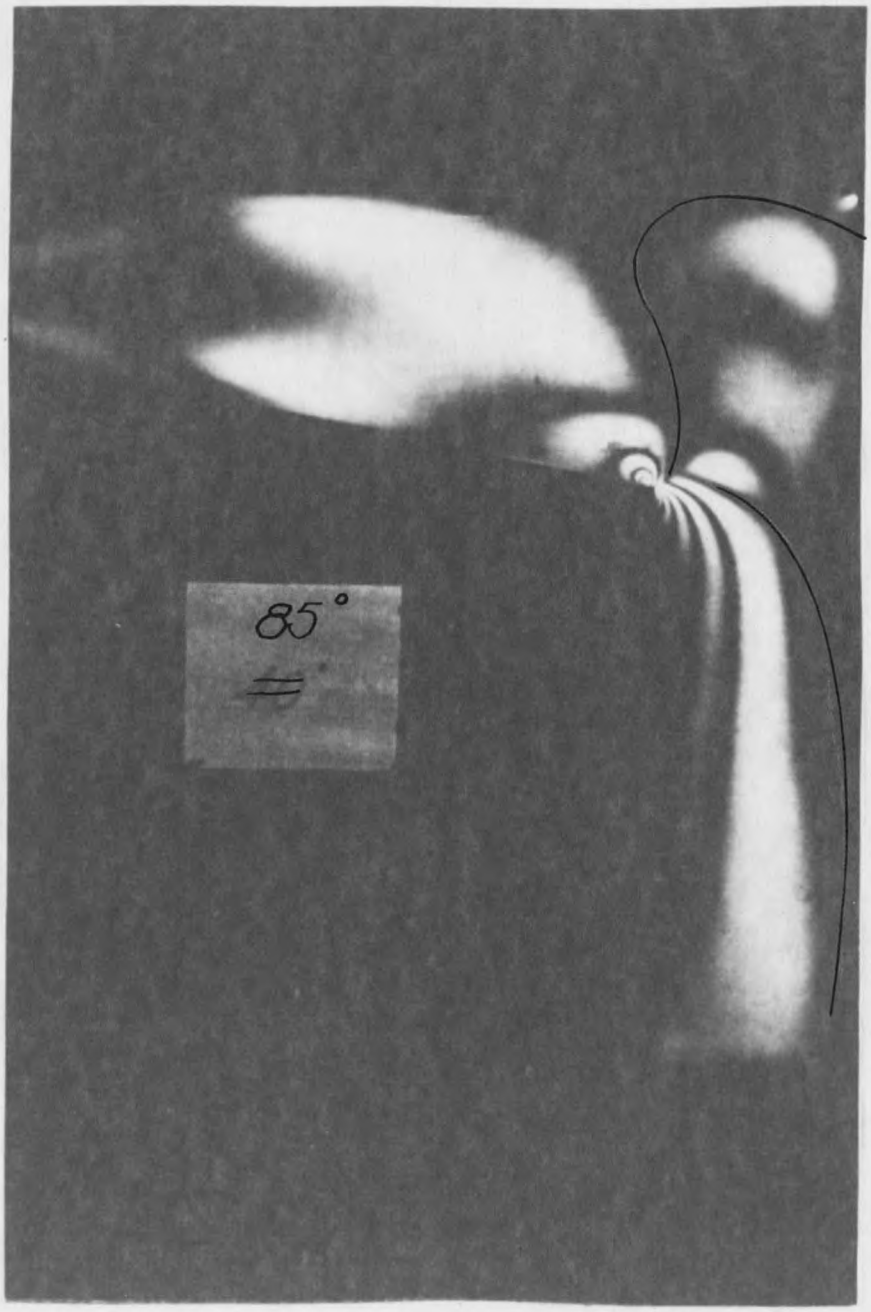
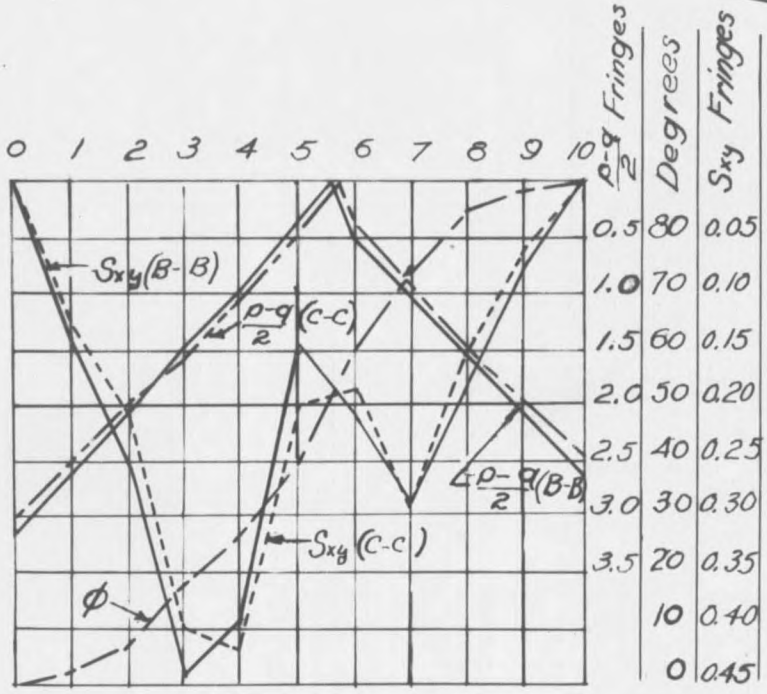
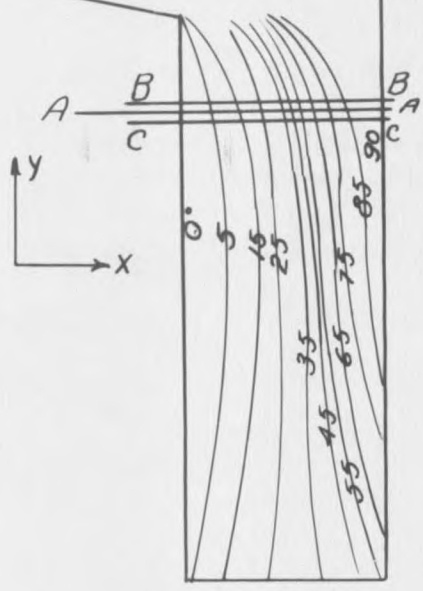


Fig. 15 85° Isoclinic Lines (Plane Setup)

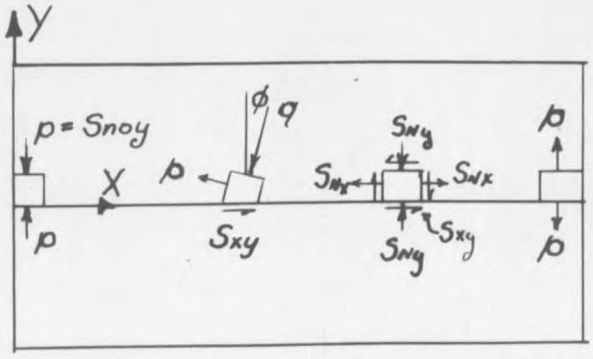


p-q/2 Fringes	Degrees	Sxy Fringes
0.5	80	0.05
1.0	70	0.10
1.5	60	0.15
2.0	50	0.20
2.5	40	0.25
3.0	30	0.30
3.5	20	0.35
	10	0.40
	0	0.45

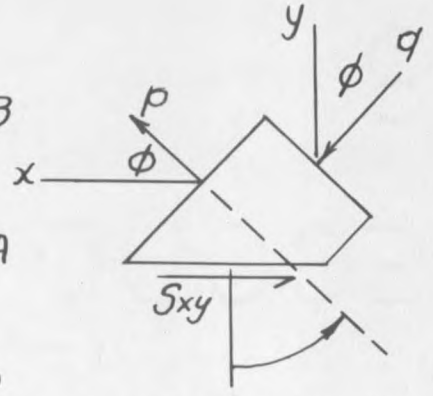
Curves Showing Variations of ϕ, Sxy, and $\frac{p-q}{2}$ for Sec. C-C and Sec. B-B
Fig. 18



Isoclinic Lines for the Column
Fig. 17



Sketch Showing Directions of Shear, Normal, and Principal Stresses
Fig. 19



Determining Shear Direction
Fig. 16

maximum principal stress, assuming tension to be positive, determines the direction of the shearing stress. If in turning the angle from the normal line to the extended maximum principal stress line a movement to the right is made, the shear stress will also be directed to the right.

The separation of the principal stresses is obtained by graphical means. (See Appendix C). This method involves solving for the normal stresses at a section and using the following relationship between principal stresses and normal stresses. (See Appendix B).

$$p = \frac{Snx + Sny}{2} \pm \sqrt{Sxy^2 + \frac{(Snx - Sny)^2}{4}} \qquad (3)$$

The normal stresses at any point, Sny and Snx, (see Fig. 19) may be evaluated from the known horizontal shear stress existing at that point and a known normal stress which is evaluated at a boundary. (See Appendix C). The relationship is as follows:

$$Sny = Snoy - \int_0^x \frac{\partial Sxy}{\partial y}\, dx \qquad (4)$$

where Sny = normal stress parallel to y axis at any point (see Fig. 19)

Snoy = known boundary stress parallel to y axis

$\int_0^x \frac{\partial Sxy}{\partial y}\, dx$ = the algebraic sum of the change in shear from the boundary point to the point being evaluated. (Approx.) See Appendix C.

The integral is solved by graphical means[12]. The following relationship is used:

$$\frac{\partial Sxy}{\partial y} \doteq \frac{(Sxy)p - (Sxy)r}{\Delta y'} \quad \text{approximately} \qquad (5)$$

12. Ibid., p. 263.

The numerator is the difference in shearing stress of two points, p and r, which lie to each side of the point being investigated, respectively. The denominator is the vertical distance between the two points p and r. The $\frac{\partial Sxy}{\partial y}$ represents the slope of the Sxy curve, if Sxy is plotted as a function of y, at the point under investigation.

The solution of the integral involves solving for the shearing stresses on two auxiliary lines which lie above and below the line under investigation. Lines B-B and C-C of Fig. 17 are the auxiliary lines and line A-A is the line under investigation.

Equation 4 may now be written:

$$Sny = Snoy = \sum_{o}^{x} \Delta Sxy \left(\frac{\Delta x}{\Delta y}\right) \qquad (6)$$

Knowing one normal stress and the shearing stress, the remaining normal stress may be found by

$$Snx = Sny \pm \sqrt{(p-q)^2 + 4Sxy^2} \qquad (7)$$

The stresses in the model were evaluated at section A-A, Fig. 17, which is 1 in. below the intersection of the column and the haunch. The stress pattern, Fig. 5, indicated that section A-A was free from the stress concentration set up at the intersection. This section was selected as the mathematical solution used does not account in full for stress concentration; therefore, in comparing the photoelastic solution and the mathematical solution a close agreement should be reached.

The shear stresses at 0.1 in. intervals for section B-B and C-C were evaluated in terms of fringes and recorded in Fig. 18 and columns 6 and 7 of Table I. The distance between lines B-B and C-C is 0.1 in.

Table I

Normal Stresses for Sec. A-A Fig. 17

Point	Sec. B-B $\frac{p-q}{2}$ Fringe	Sec. C-C $\frac{p-q}{2}$ Fringe	Sec. B-B 2ϕ Degree	Sec. C-C 2ϕ Degree	Sec. B-B Sxy Fringe	Sec. C-C Sxy Fringe	Sec. B-B - Sec. C-C $\Delta Sxy = \Delta Sxy\left(\frac{\Delta x}{\Delta y}\right)$	Sec. A-A $Snx = -\sum_{o}^{x} Sxy\left(\frac{\Delta x}{\Delta y}\right)$ Fringe	Sec. A-A Sny Fringe	Sec. A-A Snx -compression psi	Sec. A-A Sny +tension psi
0	1.6	1.55	0°	0°	0	0	0	0	-3.15	0	-1640
1	1.3	1.25	6	6	+0.136	+0.131	-0.005	-0.005	-2.545	- 3	-1320
2	1.05	1.0	14	12	+0.255	+0.208	-0.047	-0.052	-2.000	-27	-1040
3	0.75	0.80	36	30	+0.441	+0.400	-0.041	-0.093	-1.383	-48	- 719
4	0.50	0.55	52	50	+0.394	+0.422	+0.028	-0.065	-0.862	-34	- 448
5	0.15	0.20	80	74	+0.1475	+0.1925	+0.045	-0.020	-0.020	-10	- 10
6	0.25	0.20	120	114	+0.2165	+0.183	-0.0335	-0.0535	+0.1325	-28	+ 69
7	0.55	0.50	148	144	+0.291	+0.294	+0.003	-0.0505	+0.9295	-26	+ 483
8	0.80	0.80	170	168	+0.1385	+0.166	+0.0275	-0.0230	+1.547	-12	+ 804
9	1.1	1.05	176	174	+0.077	+0.1095	+0.0325	+0.0095	+2.1395	+ 5	+1110
10	1.45	1.40	180	180	0	0	0	+0.0095	+2.8095	+ 5	+1460
Col. No. 1	2	3	4	5	6	7	8	9	10	11	12

$Sxy = \frac{p-q}{2} \sin 2\phi = nF \sin 2\phi$; $\Delta x = +0.1$; $\Delta y = +0.1$; $Snx = Snox - \sum_{o}^{x} \Delta Sxy\left(\frac{\Delta x}{\Delta y}\right)$; $F = 260$ psi;

$Sny = Snx \pm \sqrt{(p-q)^2 - 4Sxy^2}$; $\quad p = \frac{Snx + Sny}{2} - \sqrt{Sxy^2 + \frac{(Snx - Sny)^2}{4}}$;

$Snox = 0$; $\quad Snoy = p$

The $\frac{p-q}{2}$ quantities are shown in Fig. 18 and were taken from the stress pattern of Fig. 5.

The expression for shearing stress in terms of fringes is developed as follows:

$$n = ct\,(p-q) \tag{1}$$

$$p-q = \frac{n}{ct} = 2Sxy_{max} \text{ (from eq. 2)}$$

and

$$Sxy = \frac{p-q}{2} \sin 2\phi \tag{2}$$

therefore

$$Sxy = nF \sin 2\phi \tag{8}$$

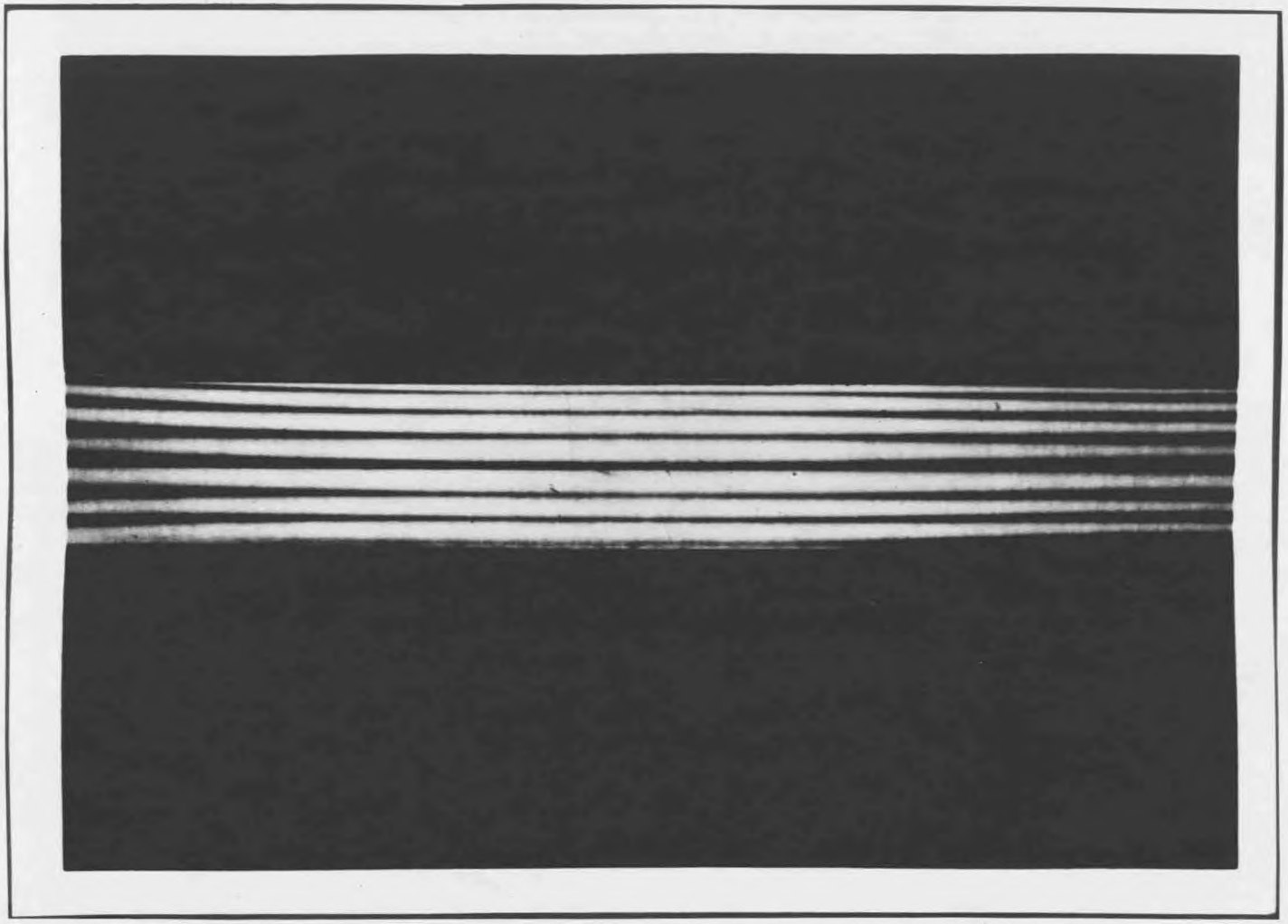
n = number of fringes
F = constant = $\frac{1}{2ct}$ (9)
ϕ = angle between the maximum principle stress and the x axis

The term F was evaluated by using a Bakelite beam (Fig. 20) to which pure bending was applied. The beam must be made from the same piece of Bakelite used for the model. This eliminates the possibility of a difference of sensitivity that might exist between two pieces of Bakelite. The stress in the beam model may be solved accurately by the bending stress formula. The fringes of the loaded beam are shown in Fig. 20. There are three fringes. The applied moment was 9.9 in. lbs. and the model was 0.4000 in. deep and 0.238 in. thick.

The maximum flexure stress in the beam is

$$S = \frac{Mc}{I} = \frac{9.9\ (0.200)}{1/12\ (.238)(.4)^3} = \frac{1.98}{0.00127} = 1560 \text{ psi.}$$

$$n = ct\,(p-q) \tag{1}$$



Fringe Pattern of Beam Under Pure Binding (Circularly Polarized Light)
Fig. 20

$3 = c\,(0.238)(1560)$; $c = 0.00809$

$$F = \frac{1}{2ct} = \frac{1}{2\,(0.00809)(0.238)} = \frac{1}{0.00385} = 260 \text{ psi.} \quad (9)$$

A sample calculation for the shear stress at point 1, Fig. 18, sec. B-B, follows and is entered in Column 6, Table I.

$$\frac{Sxy}{2} = nF \sin 2\phi = 1.3(F)(\sin 6^\circ) = 0.136\ F \text{ (Fringes)}$$

The normal stress, Snoy, parallel to the boundary on the inside of the column is known to be compression due to the type of loading. At this point the normal stress is a principal stress, Fig. 19, and its magnitude may be found as follows:

$$p-q = \frac{n}{ct} \quad (1)$$

$$F = \frac{1}{2ct} \quad (9)$$

Substituting 9 into 1

$$p-q = 2nF \quad (10)$$

$q = 0$ at boundary

Therefore,

$$p = 2nF = Snoy \quad (11)$$

$Snoy = p = 2(3.15)(260) = 1640$ psi. compression
(Col. 12, Table I)

$Snox = 0$ as only stress parallel to the boundary can exist.
(See Appendix C)

Then

$$Snx \text{ at point } 1 = Snox - \sum_{o}^{1} \Delta Sxy \left(\frac{\Delta x}{\Delta y}\right) \quad (6)$$

$$Snx_{(1)} = 0 - (+0.136 - 0.131)\,\frac{+0.1}{+0.1} = -0.005 \text{ Fringes}$$
(Col. 9, Table I)

Values of Snx were calculated in this manner for the 11 points across Sec. A-A. Knowing the Snx values for the points, the Sny values may be computed as follows:

$$Sny = Snx \pm \sqrt{(p-q)^2 + 4Sxy^2} \qquad (7)$$

Thus Sny at point 1 = $-0.005 - \sqrt{(2.55)^2 + 4(0.133)^2}$

$= -0.005 - 2.54 = -2.545$ Fringes (Col. 10, Table I)

Sny was calculated as above for each point across Sec. A-A.

Table I gives the complete solution to the normal stresses existing at 11 points across Sec. A-A. The maximum stress occurs at the inside edge of the column or point 0 and is equal to 1640 psi. compression. The magnitudes of the principal stresses across the Sec. A-A were not evaluated except at points 0 and 10 where the normal and principal stresses are equal. The design of the particular section investigated would be based upon the maximum stresses which occur at the edges.

The stress at the inside intersection of the column and girder was also computed, as at this point the stress pattern, Fig. 5, indicates maximum stress concentration. This value will be compared with the mathematical solution to illustrate the inaccuracy of the mathematical solution. Seven fringes were observed to pass through the corner. Therefore:

$$p = 2nF \qquad (11)$$

$= 2(7)(260) = 3640$ psi. compression

THE ANALYTICAL SOLUTION

The error involved in making a mathematical solution for this problem is in assuming the position of the centerline in the haunch of the girder and determining where the girder action stops and the column action begins (See Fig. 21). For this analysis, it is assumed that the column continues to the top of the bent or is 10 ft. long and 2 ft. wide. It is also assumed that the centerline of the haunch is 9 ft. above and parallel to the x-x axis of Fig. 22.

The Column Analogy method[13] is applied to obtain an analytical solution of the problem. This method is an extension of the Neutral Point Analogy[13] and the General Method of Indeterminate Structures[13].

From the Neutral Point equations the following expression can be developed to solve for the indeterminate moment:

$$Mi = \pm \left[\frac{W}{A} \pm \frac{M_{x-x}}{I_{x-x}} y \pm \frac{M_{y-y}}{I_{y-y}} x \right] \qquad (12)$$

$$W = \int \frac{M ds}{EI}$$

$$A = \int \frac{ds}{EI}$$

$$M_{x-x} = \int \frac{My ds}{EI}$$

$$I_{x-x} = \int \frac{y^2 ds}{EI}$$

y = vertical distance from the centroidal x-x axis to point under investigation.

$$M_{y-y} = \int \frac{Mx ds}{EI}$$

13. Grinter, L. E. 1947 THEORY OF MODERN STEEL STRUCTURES, The MacMillan Co., New York, Vol. II.

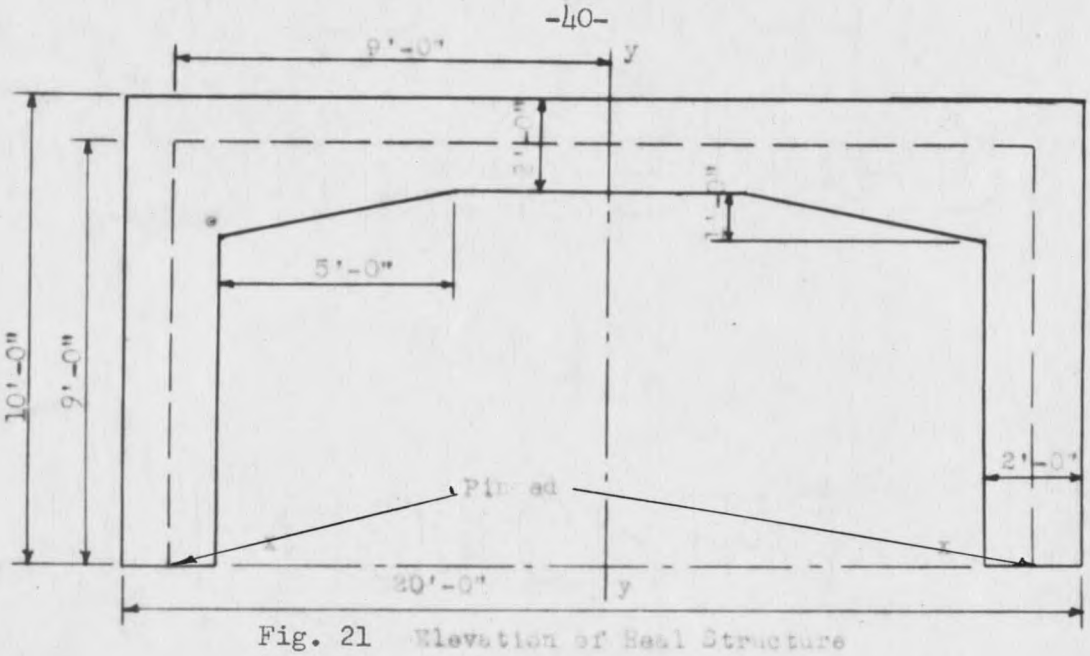


Fig. 21 Elevation of Real Structure

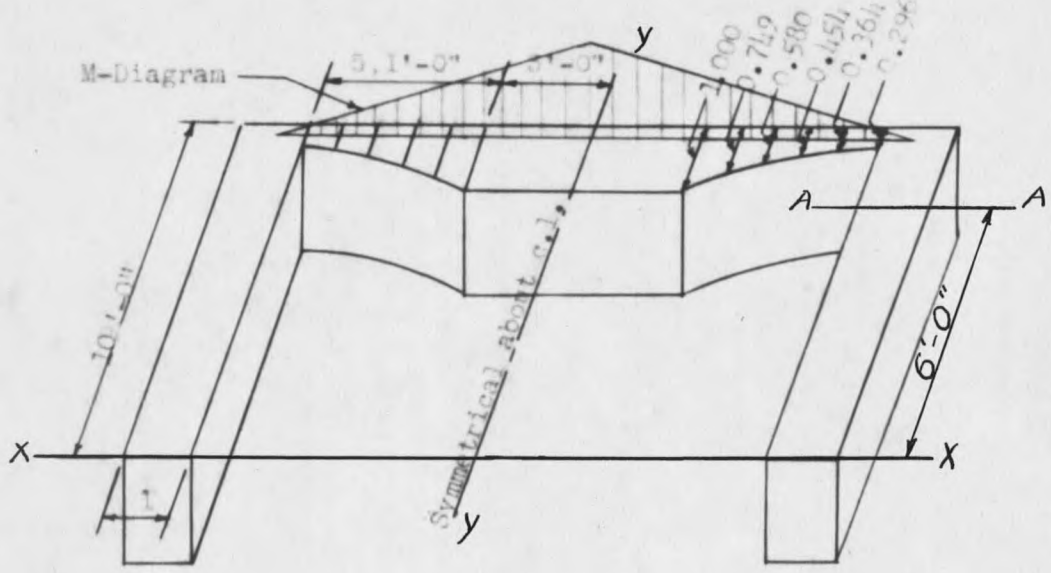


Fig. 22 Analogous Column

$$I_{y-y} = \int \frac{x^2 ds}{EI}$$

x = horizontal distance from the centroidal y-y axis to the point under investigation.

Equation 12 resembles the modified Gordon-Rankine formula[14] for eccentric loaded columns. The Gordon-Rankine formula is as follows:

$$S = \frac{P}{A} + \frac{Pdc}{I} + \frac{Pe'c'}{I'} \qquad (13)$$

From the similarity between equations 12 and 13, the Column Analogy idea is developed. The real bent is transformed into an Analogous Column by the following relationships. See Fig. 22.

$$S = Mi$$

$$P = W$$

$$A = A$$

$$Pd = M_{x-x}$$

$$I = I_{x-x}$$

$$c = y$$

$$Pe' = M_{y-y}$$

$$I' = I_{y-y}$$

$$c' = x$$

The value of A for this problem equals infinity as $\frac{1}{EI}$ for a pin is infinite. This locates the centroidal x-x axis at the pins. The y-y axis may be located by inspection due to symmetry.

The evaluation of the various terms of equation 12 follow. These

14. Laurson, P. G. and Cox, W. J. 1947 MECHANICS OF MATERIALS, John Wiley and Sons, New York.

terms are for the Analogous Column.

$I_{y-y} = \int \frac{x^2 dx}{EI}$ = inertia of columns + inertia of haunch segments + inertia of uniform depth of girder = $10(1)(2)(9)^2 + \frac{(0.296 + 0.364)}{2}(1)(2)(7.5)^2 + \frac{(0.364 + 0.454)}{2}(1)(2)(6.5)^2 + \frac{(0.454 + 0.580)}{2}(1)(2)(5.5)^2 + \frac{(0.580 + 0.749)}{2}(1)(2)(4.5)^2 + \frac{(1.000 + 0.749)}{2}(1)(2)(3.5)^2 + \frac{1}{12}(1)(6)^3 =$

$1620 + 37.1 + 34.5 + 31.3 + 26.8 + 21.1 + 18 = 1789$ (approx.)

I_{x-x} (Assumed 9 ft. to centerline of each segment of girder) = $\int \frac{y^2 ds}{EI}$ = inertia of columns + inertia of haunch segments + inertia of uniform depth of girder = $2/3\ (1)(10)^3 + (0.660)(9)^2 + 0.818(9)^2 + 1.034(9)^2 + 1.329(9)^2 + 1.749(9)^2 + 6(9)^2 =$

$666 + 53.5 + 66.2 + 83.9 + 107.5 + 141.5 + 486 = 1605$ (approx.)

$W = \int \frac{M ds}{EI}$ = summation of static moment times area of each segment of column = $\frac{P}{2}\frac{(6 + 9)}{2}(6) + \frac{P}{2}(1.5)(.660) + \frac{P}{2}(2.5)(8.18) + \frac{P}{2}(3.5)(1.034) + \frac{P}{2}(4.5)(1.329) + \frac{P}{2}(5.5)(1.749) =$

$22.5P + 0.49P + 1.02P + 2.33P + 4.81P = 31.2P$ (approx.)

$M_{x-x} = \int \frac{My\,ds}{EI}$ = moment of W of each segment about the x-x axis =

$22.5P(9) + 0.49P(9) + 1.02P(9) + 2.33P(9) + 4.81P(9) =$

$202P + 4.4P + 9.2P + 20.9P + 43.3P = 279.8P$

$M_{y-y} = \int \frac{Mx\,ds}{EI} = 0$ (Symmetry)

From equation 12, Mi at Sec. A-A (Fig. 22) is as follows:

$$Mi = \pm \left[\frac{31.2P}{\infty} \pm \frac{279.8P(6)}{1605} \pm \frac{(0)(9)}{1728}\right] = \pm 1.045P$$

The flexure stress caused by this moment at Sec. A-A in the model with P equal to 58 lbs. is as follows:

$$S = \frac{Mc}{I} = \frac{1.045\ (58)(0.5)}{1/12\ (0.23)(1)^3} = \pm 1585 \text{ psi.}$$

There is also direct stress at Sec. A-A and is equal to:

$$S = \frac{P}{A_{A-A}} = \frac{29}{(0.23)(1)} = -126 \text{ psi. compression}$$

The total combined stresses on the edges of the real column are:

$\pm 1585 - 126 = -1711$ psi. compression inside + 1459 psi. tension outside

The value of the stress at the inside intersection of the column and girder was also computed.

$$Mi = \frac{M_{x-x}}{I_{x-x}} y = \frac{280P(7)}{1605} = 1.22P$$

$$S = \frac{Mc}{I} = \frac{-1.22(58)(0.5)}{1/12\ (0.23)(1)^3} - 126 = -1850 - 126 = -1976 \text{ psi. compression}$$

CONCLUSION

Upon completion of the thesis, several improvements to the laboratory apparatus become apparent. A universal loading frame should be constructed. This would eliminate the present method of constructing a loading frame for each problem. It would be advantageous to incorporate appropriate lenses so the image of the stressed model could be projected upon a screen. Group study could more easily be handled with the image viewed on the screen. A firm polishing wheel and a milling machine would

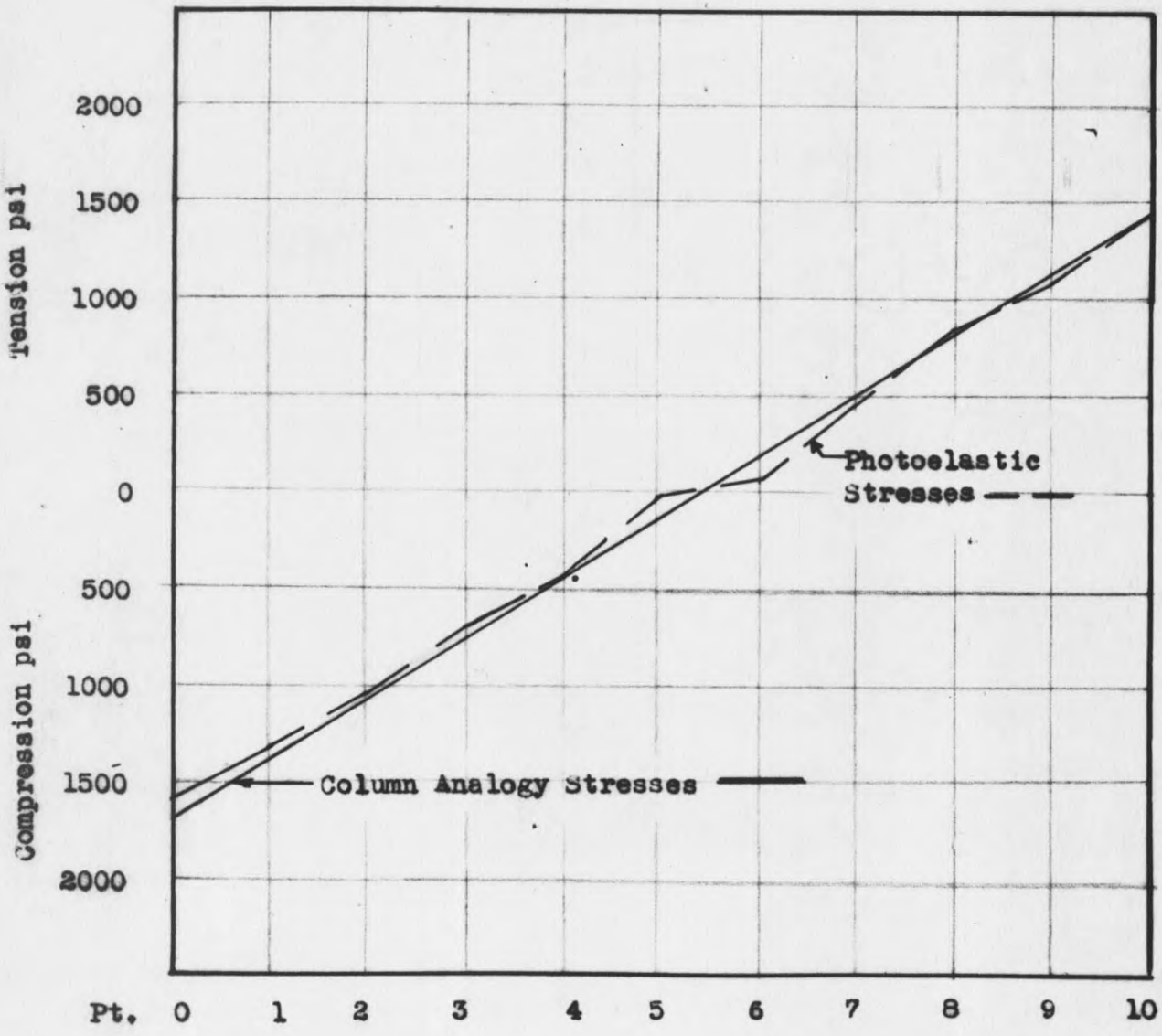
greatly reduce the time in preparing the model. They would also help reduce the error introduced by hand polishing.

The photoelastic solution under the most ideal conditions is still subject to some error. The model material may not have all the properties[15] that the ideal material should have. There is error in interpreting the photographs, such as evaluating the fraction of fringes existing at a point, or measuring the ϕ angle from the isoclinic lines. Errors are also caused by lack of perfect agreement with the light theory, i.e., the lenses may not be exactly parallel, their optic axis not exactly crossed, or the model may not intercept the light at exactly a right angle. Therefore, it must be remembered that the results are not precise. However, as mentioned earlier in the thesis, photoelasticity often gives a truer picture of internal stresses than the mathematical theory and it can save considerable time on extremely complicated stress problems.

Using the photoelastic stress analysis as a basis for comparison, very close results were obtained for the investigated section. Fig. 23 shows the variation in stress as computed by the two methods. The Column Analogy gave a maximum compressive stress that was 4.33% different than obtained by photoelasticity and the maximum tensile stress values agreed. The maximum stress values are the controlling points in design and therefore are of the greatest interest.

It is thus seen that while numerous sources of error existed, the

15. Frocht, M. M. 1941 op. cit., p. 323.



Comparisom of Stresses
Fig. 23

composite effect of such errors is well within the accuracy of the accepted engineering design calculations.

At the inside intersection of the column and girder, where stress concentrations not accounted for by the column analogy occur, 3640 psi. was found by photoelasticity and only 1976 psi. was found by Column Analogy. This difference was 46%. Therefore, in structures where stress concentrations may be serious it seems wise to make a model analysis.

APPENDIX A

Light Theory as it Pertains to Photoelasticity

There are several theories advanced to explain light. The most useful theory to explain photoelasticity is the light wave theory[16]. Some of the main properties of light pertaining to photoelasticity will be presented.

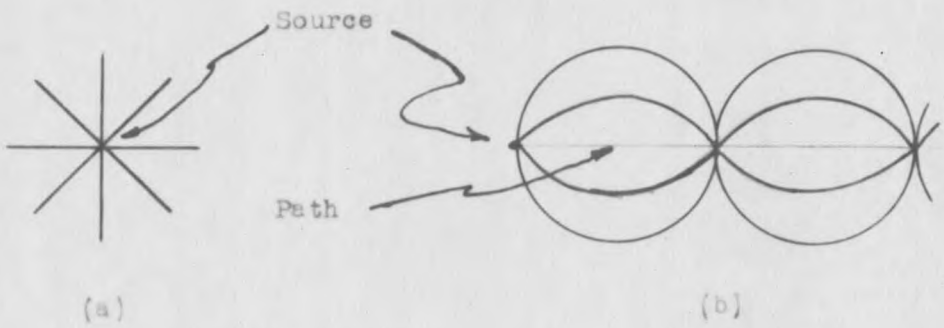
If a light source usually found in use is explained in terms of waves, it must be imagined that the waves vibrate in all planes passing through the point source[17]. (See Fig. A-1). The vibrating particles do not travel in the direction in which the wave is traveling but rather in a direction transverse to the direction of propagation. White light consists of waves having different lengths and amplitudes. A definite wave length is needed to make a quantitative result in photoelasticity; therefore, the light is filtered to obtain light of one color or wave length.

Plano-polarized light consists of light waves vibrating in one plane. (See Fig. A-2). The most common method used to obtain plano-polarized light is to pass light through a commerical material called polaroid.

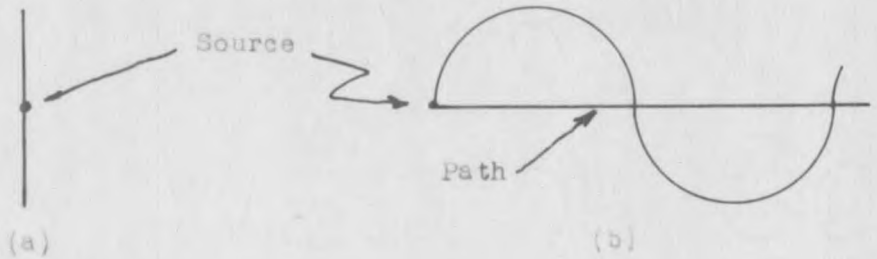
All homogeneous transparent bodies have the characteristic of altering the path of light when it is passed through them. This phenomenon is called single refraction. It may be observed that the original path is deflected away from the perpendicular to the boundary of the medium which

---

16. Alexander, N. 1936 PHOTOELASTICITY, Rhode Island State College, p. A-3.
17. Robertson, John Kellock F.R.S.C. 1935 INTRODUCTION TO PHYSICAL OPTICS, D. VanNostrand Co., Inc., New York.



Unpolarized Light
Figure A-1



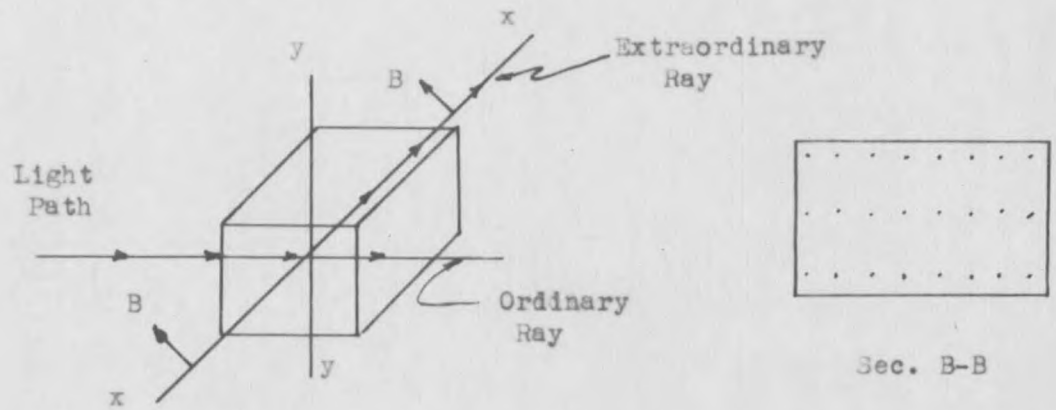
Polarized Light
Figure A-2

is less dense. Materials used in photoelasticity models are single refracting when unstressed.

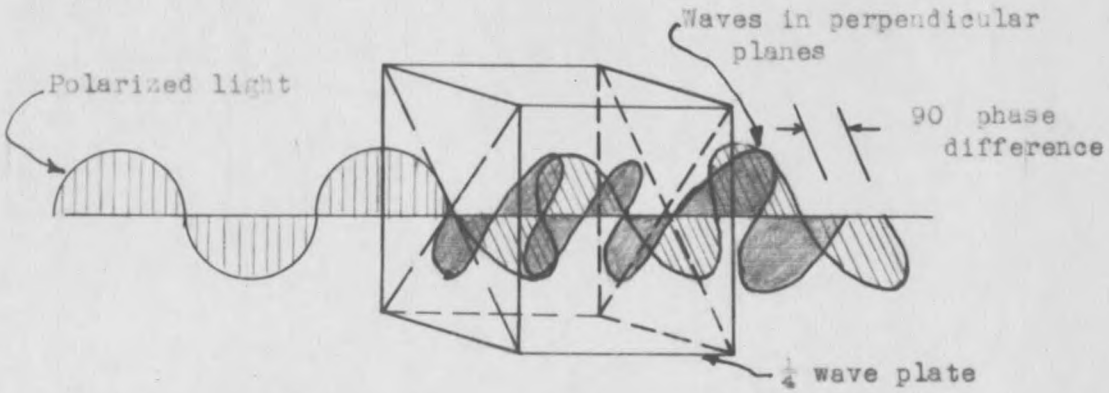
Double refraction of light occurs in some bodies when light is passed through them. This is considered to mean a light wave is split into two paths within the body, for example, the behavior of light passed through a Nicol prism. (See Fig. A-3). It may also mean a light wave is split into two waves which are in mutually perpendicular planes but have the same path of propagation. (See Fig. A-4). The position of the optic axis of the material will determine the type of double refraction that will take place. If plano-polarized light is passed through a double refracting body, the light emerging will also be plano-polarized regardless of the position of the optic axis.

The refracting properties may be explained if a body is thought of as consisting of particles forming right angle rows to each other. (See Fig. A-3). The spacing in the vertical direction is larger than the spacing in the horizontal direction. If it is assumed that the particles provide resistance to the passage of the waves, the particles farther apart will more readily pass the waves than those closer together.

The photoelasticity model material which is homogeneous and single refracting when unstressed will assume double refracting characteristics when stressed. The reason is explained by the separation of the particles causing a difference in resistance to light passage in perpendicular planes. The optic axis of the model material is in the plane of the model and will split the light wave into two waves in mutually perpendicular



Double Refraction
* Figure A-3



Function of Quarter-Wave Plate
* Figure A-4

* All figures suggested or duplicated from Photoelasticity by N. Alexander

planes with each having the same path of propagation. (See Fig. A-5).

When polarized waves pass through a body and each wave is split into two waves in mutually perpendicular planes and with one wave retarded one-fourth of a wave length, the body is a quarter-wave plate. Photoelasticity terminology calls this light circularly-polarized. (See Fig. A-4).

If polarized monochromatic light is passed through a stressed body, the double refraction mentioned previously will take place. The two waves in mutually perpendicular planes may be out of phase or one retarded with respect to the other. The amount of retardation will depend upon the intensity of the stress at the point of passage of the light. (See Fig. A-5).

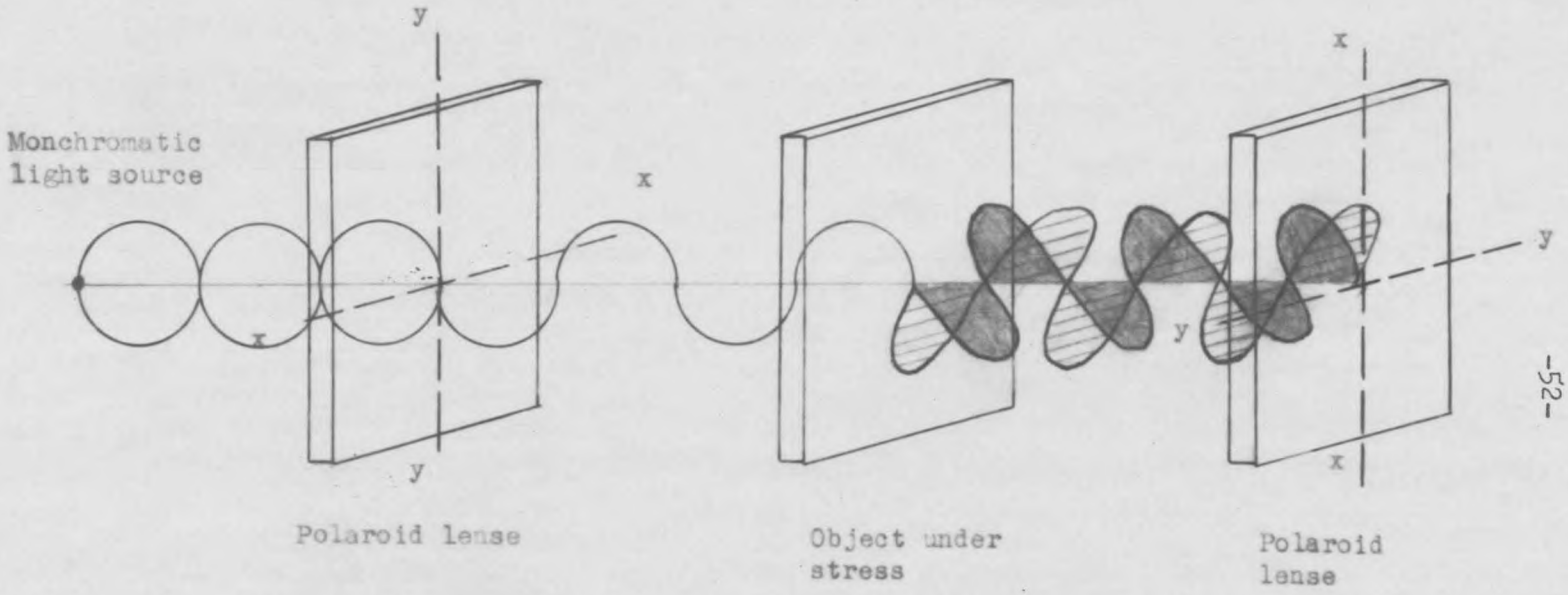
If the unstressed object is viewed by eye when the object is between two crossed polaroid lenses, it will be dark. Upon application of the load to the object, light and dark bands will appear. The light bands are the result of two waves which support each other and the dark bands may be the result of two waves being entirely out of phase and cancelling each other, or it may be that the waves are in planes perpendicular to the second polaroid optic axis. The retardation or difference in phase may be expressed by the following equation[18]:

$$R = clt \qquad \text{(A-1)}$$

where

R = the retardation of the wave
c = a constant depending on the material and light used
l = the stress condition
t = the thickness of the material

18. Alexander, N. op. cit., p. C-6.



Crossed Polaroid Lenses
Figure A-5

To correlate the definitions presented, the path of a light wave will be followed through a plane photoelastic setup. (See Fig. A-5). The light is first filtered to obtain monochromatic light. This light wave is passed through the polaroid lense to confine the vibrations to one plane. The light next passes through the stressed object and undergoes double refraction. The two mutually perpendicular planes are also planes containing the principal stresses. One wave is retarded with respect to another and the amount of retardation depends upon the difference in principal stresses. The light next encounters the second polaroid lens and only waves or components of the waves parallel to the optic axis of the second lens will pass. There will be some waves which are perpendicular to the optic axis of the second lens and hence none of the waves will pass. This fact is taken advantage of to plot isoclinic lines. As all stressed points causing waves to be perpendicular to the optic axis of the second polaroid lens also have principal stresses perpendicular to the optic axis of the second polaroid lens, a locus of similar points may be plotted. The locus of points are recorded to indicate the lines of principal stresses having the same plane of inclination.

To eliminate the isoclinic lines a modification is added to the plane setup. A quarter-wave plate (Fig. A-4) is added on each side of the stressed model. Using the same light wave as in the plane setup, the light emerging from the quarter wave will be doubly refracted with one wave retarded $\frac{1}{4}$ wave length with respect to the other. The vibration of the

particles now will describe circular motion[19]. The light under circular motion will now pass through the principal stress planes of the model and emerge with circular motion or elliptical motion. This motion is converted into plano-polarized vibrations by the second $\frac{1}{4}$ wave plate and the second polaroid plate analyzes as before. A fringe viewed from this setup is a locus of points along which the difference in principal stresses is constant.[20]

19. Robertson, J. K. op. cit., p. 314.
20. Frocht, M. M. 1941 op. cit., p. 131.

APPENDIX B

Stress Relations as They Pertain to Photoelasticity

In a prismatic bar loaded under a tension load it is usually assumed that the stress parallel to the direction of the applied load on any cross section in the bar is equal to the following expression. (See Fig. B-1).

$$S_{a-a} = \frac{F}{\text{area of section a-a}} = \frac{F}{Ax/\cos \phi} = \frac{F \cos \phi}{Ax} \qquad (B-1)$$

where Ax is the area perpendicular to the load.

$$S_x = \frac{F}{Ax} \qquad (B-2)$$

if Sx is the stress perpendicular to the section Ax. Then,

$$S_{a-a} = S_x \cos \phi \qquad (B-3)$$

We see that S_{a-a} is a maximum when $\phi = 0^\circ$ and a minimum when $\phi = 90^\circ$. S_{a-a} may be divided into components, one parallel and one perpendicular to section a-a. The component parallel to the section is termed shear stress and the component perpendicular is known as the normal stress. (See Fig. B-2). The normal stress may be written:

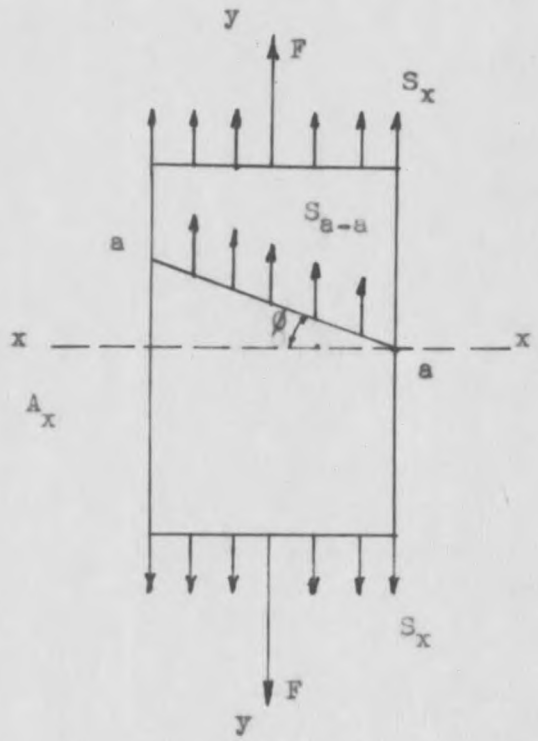
$$S_n = S_{a-a} \cos \phi = Sx \cos \phi \cos \phi = Sx \cos^2 \phi, \text{ or}$$

$$S_n = S_x \frac{1 + \cos 2\phi}{2} \qquad (B-4)$$

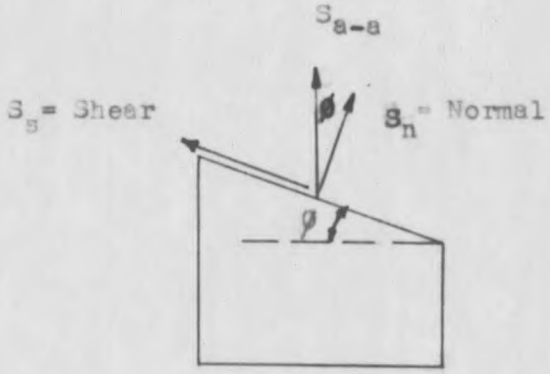
The shearing stress may be written:

$$S_s = S_{a-a} \sin 2\phi = S_x \sin \phi \cos \phi = S_x \frac{\sin 2\phi}{2} \qquad (B-5)$$

From the equation B-4 it can be seen that S_n is maximum when $\phi = 0^\circ$ and minimum when $\phi = 90^\circ$. By similar reasoning the maximum S_s occurs when $\phi = 45^\circ$ and is minimum when ϕ is 0° or 90°.



Tension Bar
* Figure B-1



Components of S_{a-a}
*Figure B-2

* All figures suggested or duplicated from Photoelasticity by N. Alexander.

By taking an isolated element from the tension specimen, the following relationship between normal and shear stresses may be obtained. (See Fig. B-3).

$$S_n = S_x \cos^2 \phi \qquad S_s = S_x \frac{\sin 2\phi}{2}$$

$$S_n' = S_x \cos^2 \phi' \qquad S_s' = S_x \frac{\sin 2\phi'}{2}$$

If the above expressions are added and observing $\phi + \phi' = 90^\circ$ or $\phi' = 90^\circ - \phi$ and $\cos \phi' = \sin \phi$, the following equations result:

$$S_n + S_n' = S_x \cos^2 \phi + S_x \cos^2 \phi' = S_x = S_n \text{ max.} \quad \text{(B-6)}$$

$$\sin 2\phi' = \sin 2(90^\circ - \phi) = \sin (180^\circ - 2\phi) = \sin 2\phi$$

$$S_s = S_x \frac{\sin 2\phi}{2} \qquad S_s' = S_x \frac{\sin 2\phi'}{2}$$

$$S_s = S_s' \quad \text{(B-7)}$$

The following conclusions are forthcoming:

1. The sum of the normal stresses is constant and equal to S_n max.
2. The shearing stresses are of equal magnitude.

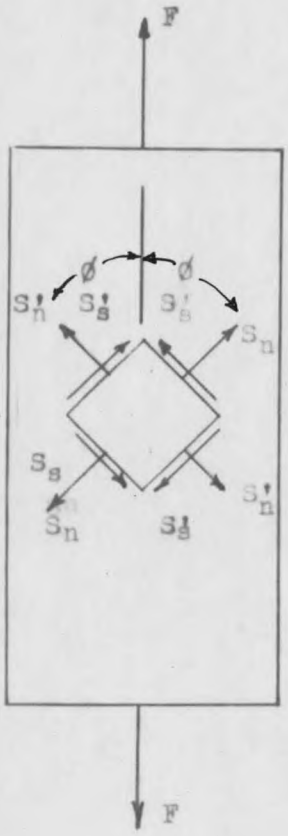
Consider a bar subjected to tensile forces in two perpendicular directions. (See Fig. B-4). The foregoing analogy may be applied and the following results obtained.

$$S_x = \frac{F_x}{A_x} \qquad S_y = \frac{F_y}{A_y}$$

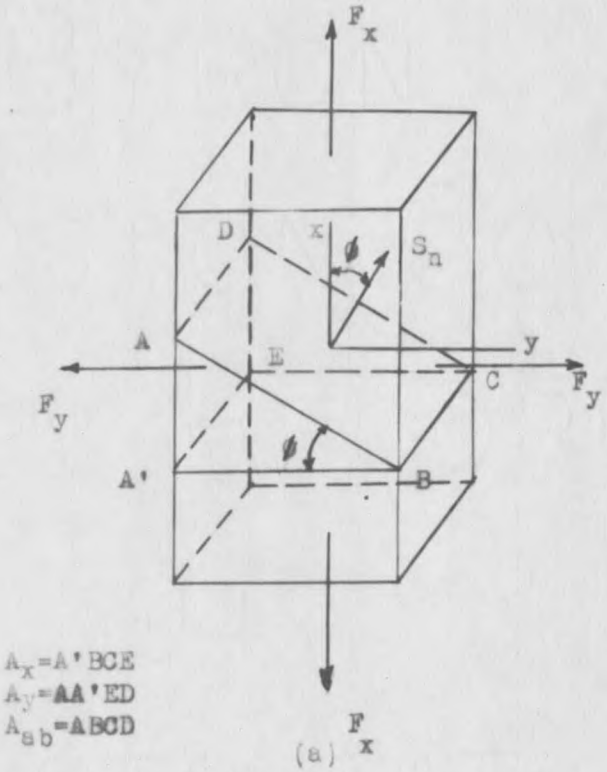
$$A_x = A_{ab} \cos \phi = A'BCE$$

$$A_y = A_{ab} \sin \phi = AA'ED$$

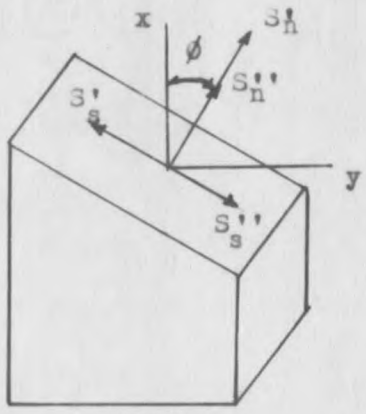
$$A_{ab} = \frac{A_x}{\cos \phi} = \frac{A_y}{\sin \phi} = ABCD$$



Tension Bar and
Element Selected at Random
* Figure B-3



(a)



(b)

Combined Tensions
* Figure B-4

* All figures suggested or duplicated from Photoelasticity by N. Alexander.

Normal stresses on plane AB

$$S_n' = \frac{F_x}{A_x} \cos^2 \phi \qquad S_n'' = \frac{F_y}{A_y} \sin^2 \phi$$

$$S_n' + S_n'' = S_n = \frac{F_x}{A_x} \cos^2 \phi + \frac{F_y}{A_y} \sin^2 \phi$$

$$S_n = S_x \cos^2 \phi + S_y \sin^2 \phi \qquad \text{(B-6)}$$

Shear stresses on plane AB

$$S_s' = \frac{F_x}{A_x} \frac{\sin 2\phi}{2} \qquad S_s'' = \frac{F_y}{A_y} \frac{\sin 2\phi}{2}$$

$S_s' = S_s''$ (notice opposite signs)

$$S_s = S_s' - S_s'' = \frac{F_x}{A_x} - \frac{F_y}{A_y} \frac{\sin 2\phi}{2}$$

$$S_s = \frac{S_x - S_y}{2} \sin 2\phi \qquad \text{(B-8)}$$

When ϕ is 0° or 90° the normal stresses reach a maximum or minimum value and the shear stress equals zero. The maximum shear stress occurs when $\phi = 45^\circ$. The normal stresses shall be called principal stresses and the directions principal stress directions when ϕ is 0° or 90°.

Investigating a thin beam subjected to a coplanar force system (See Fig. B-5), S_n and S_s can be calculated since S_s', S_s'', S_n' and S_n'' are known. The forces acting on the three sides of the element are:

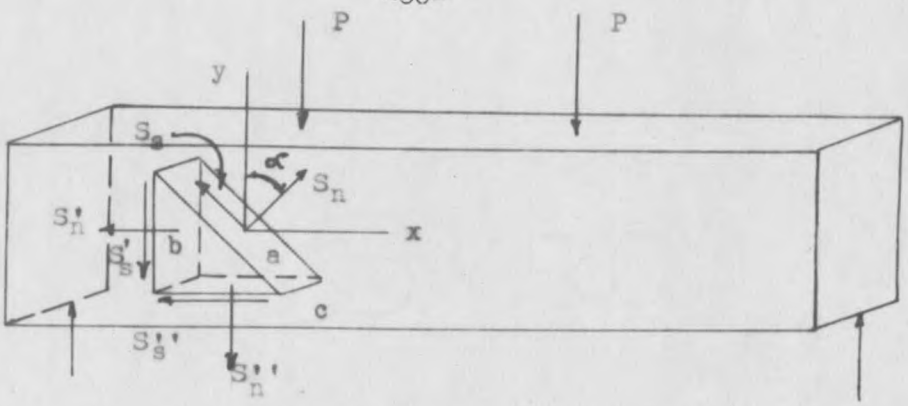
$$S_n A_a = S_n'' A_c \cos\alpha + S_n' A_b \sin\alpha + S_s'' A_c \sin\alpha + S_s' A_b \cos\alpha$$

$A_c = A_b$ (areas marked on figure B-5)

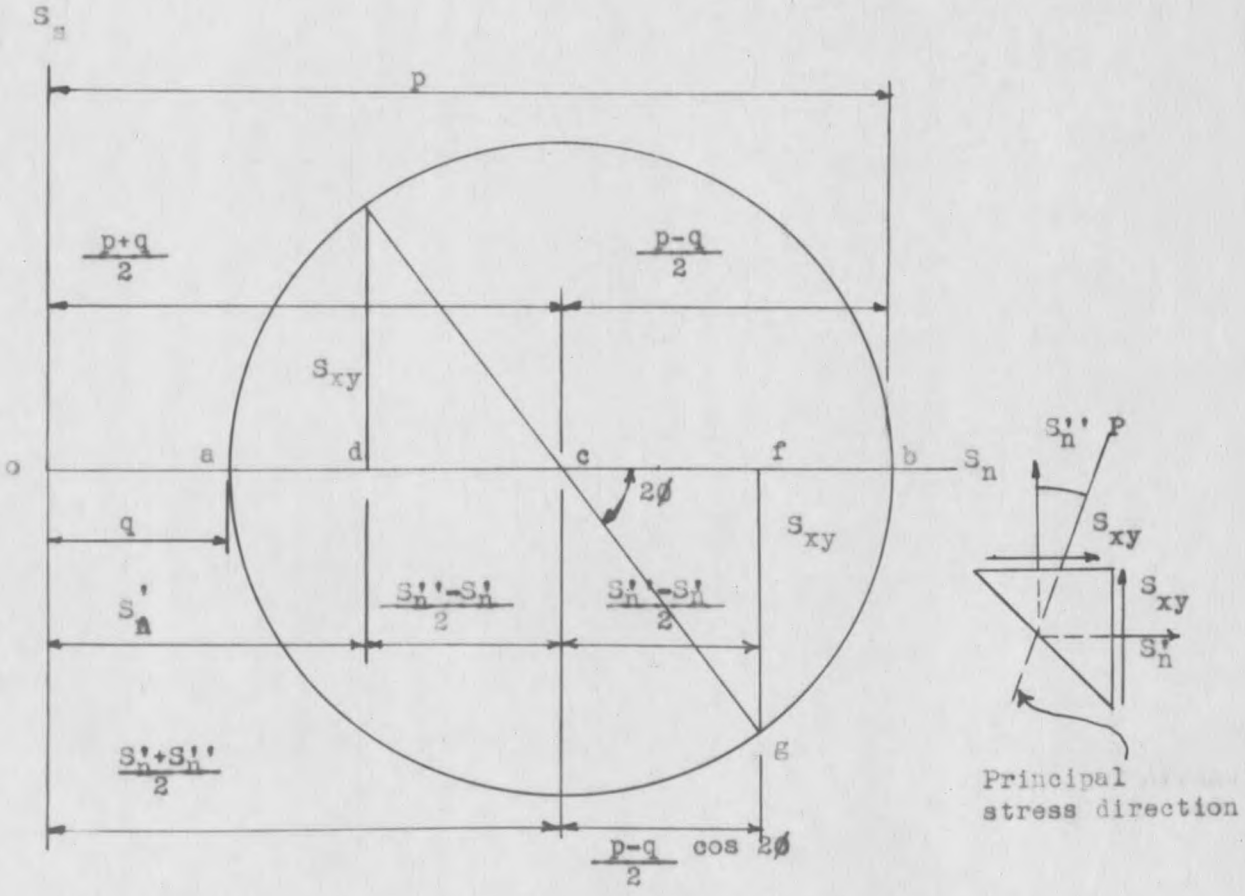
$$S_s A_a = S_n'' A_c \sin\alpha - S_n' A_b \cos\alpha - S_s'' A_c \cos\alpha + S_s' A_b \sin\alpha$$

$S_s' = S_s'' = S_{xy}$ $\qquad A_b = A_a \sin\alpha$ $\qquad A_c = A_a \cos\alpha$

$$S_n = S_n'' \cos^2\alpha + S_n' \sin^2\alpha + S_{xy} \sin 2\alpha \qquad \text{(B-9)}$$



Element in Simple Beam
Figure B-5



Sketch Showing Determination of Principal Stresses (Mohr's Circle)
* Figure B-6

* All figures suggested or duplicated from Photoelasticity by N. Alexander.

$$S_s = S_{xy} (\sin^2\alpha - \cos^2\alpha) + \frac{S_n' - S_n''}{2} \sin 2\alpha \qquad \text{(B-10)}$$

The two equations, B-9 and B-10, can be used to calculate the normal and shear stresses at any point in the beam if the components S_n', S_n'', and S_{xy} are known. The element previously considered may be selected in such a manner that S_{xy} will be zero. Solving equation B-10 with S_s equal to zero, the following is obtained:

$$\frac{S_{xy}}{S_n'' - S_n'} = \frac{1}{2} \tan 2\phi \quad (\alpha = \phi) \qquad \text{(B-11)}$$

This expression gives us two angles in which there will be zero shear. The two directions are called principal stress directions and the normal stresses are called principal stresses. When the principal stresses are found, one will be at its maximum value and one at its minimum value. If the x and y axis of Fig. B-5 are oriented to the principal stress directions equations B-9 and B-10 reduce to:

$$S_n = p \cos^2 \theta + q \sin^2 \theta \qquad \text{(B-12)}$$

$$S_s = \frac{(p-q) \sin 2\theta}{2} \qquad \text{(B-13)}$$

$p = S_n''$ $\quad q = S_n'$ (p and q are the principal stresses)

θ = angle measured from principal stress directions

With the following equations, the principal stresses may be calculated if the S_n', S_n'', and S_{xy} values are known for any element.

$$p = \frac{S_n'' + S_n'}{2} + \sqrt{S_{xy}^2 + \frac{(S_n'' - S_n')^2}{4}} \qquad \text{(B-14)}$$

$$q = \frac{S_n'' + S_n'}{2} - \sqrt{S_{xy}^2 + \frac{(S_n'' - S_n')^2}{4}} \qquad \text{(B-15)}$$

Equations B-14 and B-15 will be proven by the Mohr circle. (See Fig. B-6). The horizontal axis represents principal stresses at a particular point. p = ob and q = oa. The vertical axis represents shear stresses. Line ab represents p - q. The distances od and of represent S'_n and S''_n acting on two right-angled planes. The lines de and fg are the shear stresses S_{xy} acting on these planes.

$$of = oc + cf = \frac{p + q}{2} + (cg)(\cos 2\phi)$$

$$S''_n = \frac{p + q}{2} + \frac{p - q}{2} \cos 2\phi \qquad \text{(B-16)}$$

which reduces to:

$$S''_n = p \cos^2 \phi + q \sin^2 \phi \qquad \text{(B-17)}$$

$$cg = \frac{p - q}{2}; \quad gf = cg \sin 2\phi$$

$$gf = S_{xy} = \frac{p - q}{2} \sin 2\phi \qquad \text{(B-18)}$$

$$cg = \sqrt{(fg)^2 + (cf)^2} \qquad fg = S_{xy} \qquad cf = \frac{S''_n - S'_n}{2}$$

It is seen that

$$ob = oc + cb = oc + cg \qquad ob = p \qquad oc = \frac{S'_n + S''_n}{2}$$

which gives us

$$p = \frac{S'_n + S''_n}{2} + \sqrt{S^2_{xy} + \frac{(S''_n - S'_n)^2}{4}} \qquad \text{(B-19)}$$

also:

$$oa = oc - ca = oc - cg$$

therefore:

$$q = \frac{S'_n + S''_n}{2} - \sqrt{S^2_{xy} + \frac{(S'_n - S''_n)^2}{4}} \qquad \text{(B-20)}$$

By adding the above two expressions for principal stresses a proof is obtained showing the sum of the principal stresses are always equal to the sum of the normal stresses or:

$$S_n' + S_n'' = p + q$$

APPENDIX C

Photoelastic Analysis of Stresses

There are several methods developed on the determination of stresses by photoelasticity. The method used in this thesis is called the Shear Difference Solution[21]. It makes use of the stress optic law and the isoclinic lines in the model.

The first portion of the solution is to solve for the difference in principal stresses by the stress optic law. The stress optic law is (See Appendix A):

$$n = ct\,(p - q) \qquad (A\text{-}1)$$

n = the retardation or fringe order

c = a constant depending upon the material and light source used

t = thickness of the model

(p - q) = the difference between the principal stresses

The retardation of light is an indication of stress intensity. The difference in principal stress may be of such a magnitude that it causes the light waves emitted from the model to be out of phase one wave length or some even multiple of one wave length. This will cause complete darkness at that particular stressed point in the model.

For an example, consider a beam having pure bending applied for a load. The stress at the extreme fibers will be maximum and at the neutral axis zero. (See Fig. C-1). Between the two extremes there is a straight

---

21. Frocht, M. M. 1941 op. cit., p. 252.

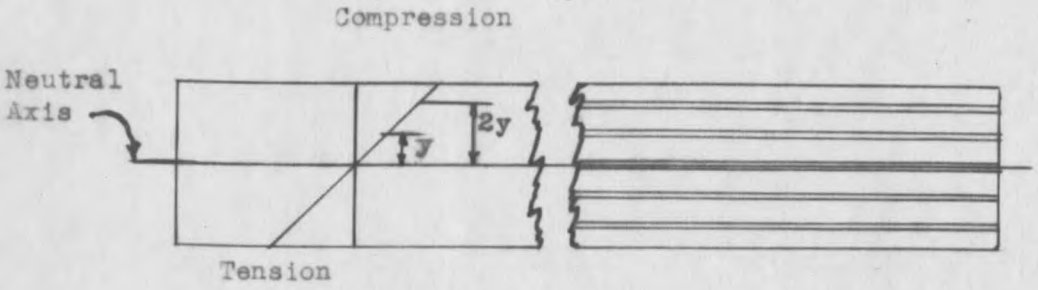
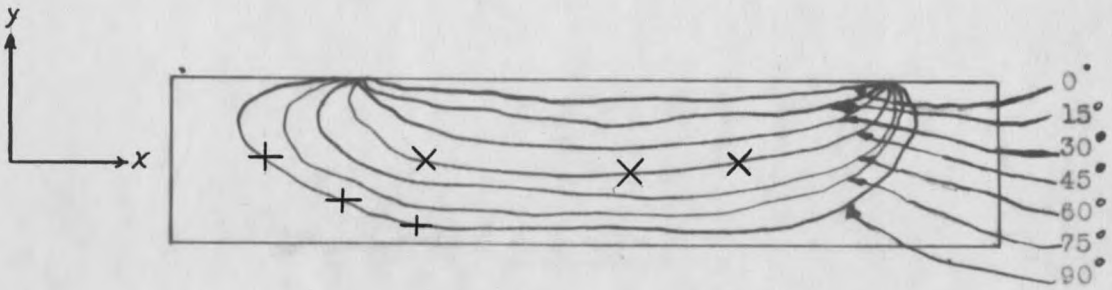


Diagram of Beam Under Pare Bending
Figure C-1



Isoclinics on a Beam Under Pure Bending
Figure C-2

line variation of stress. If the beam is placed in monochromatic circularly polarized light, there will be fringes or alternating dark and light bands of color between the neutral axis and the edges of the beam. (See Fig. C-1). The dark bands or fringes are a locus of points at which the difference between the principal stresses is constant. The fringe is also a locus of points of equal maximum shear stresses. (See Appendix B).

If the model is loaded in monochromatic circularly polarized light and a picture is taken of the fringes or stress pattern, the difference between the principal stresses may be found by equation A-1. Available data will give us the constant of the material and light and the thickness of the model can be measured.

The next step is to separate the principal stresses. This is accomplished in part by a graphical solution. Usually the variation in principal stresses is required for a definite cross section in the model. The Shear Difference Solution calls for computing the shear stresses on parallel lines a small distance apart. These lines are to either side of the original line under investigation. The shear stresses are found by the following equation (See Appendix B):

$$S_{xy} = \frac{p - q}{2} \sin 2\phi \qquad \text{(B-13)}$$

$\frac{p - q}{2}$ = the difference in principal stresses found by equation A-1

ϕ = the angle the maximum principal stress makes with the x axis

In order to find ϕ, isoclinic lines are used. An isoclinic is a locus of points along which the principal stresses have parallel directions and

are of constant magnitude.[22] (See Fig. C-2)

If the loaded model is placed between crossed polaroid lenses, dark lines will be seen in the model. When the crossed lenses are rotated, some of the dark lines or isoclinics will appear to rotate. The lines which rotate are the isoclinic lines. (See Appendix A).

By rotating the two crossed lenses through 0°, 10°, 20°, etc., a system of isoclinics may be plotted. The angles are correlated with the optic axes of the lenses. With the lenses crossed, the x axis is marked to correspond to the optic axis of the first lens and this axis is used as a reference for measuring ϕ. The shear stresses may now be calculated for any point.

An expression will be developed relating the normal and shear stresses at a point. Once the normal stresses are found, the principal stresses can be evaluated. (See Appendix B).

The relationship between normal and shearing stresses follows (See Fig. C-3):[23]

Neglecting the width $F_x = 0$

$$\left(S_n' + \frac{\partial S_n' dx}{\partial x}\right)dy - S_n' dy + \left(S_{xy} + \frac{\partial S_{xy} dy}{\partial y}\right)dx - S_{xy} dx = 0$$

which reduces to:

$$\frac{\partial S_n'}{\partial x} + \frac{\partial S_{xy}}{\partial y} = 0 \qquad (C\text{-}1)$$

$F_y = 0$

22. Ibid., p. 177.
23. Alexander, N. op. cit., p. C-21.

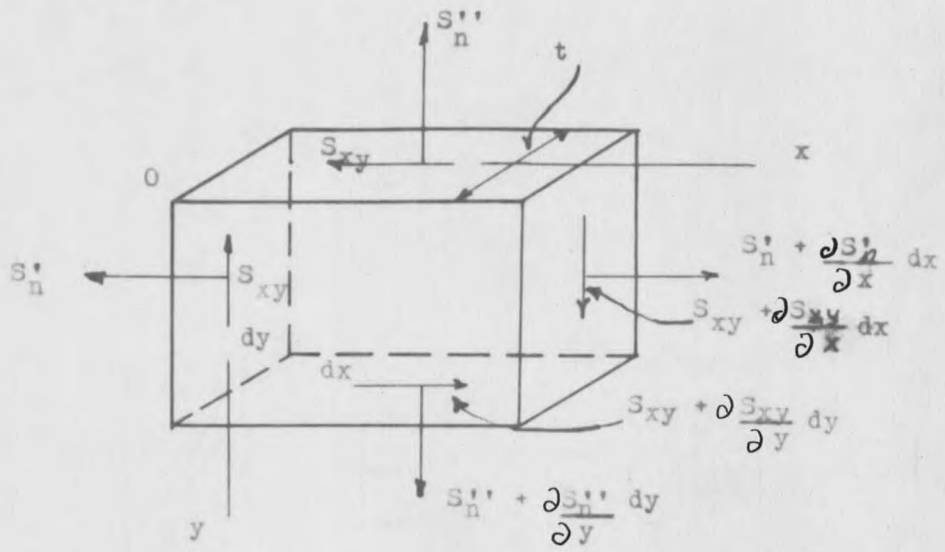
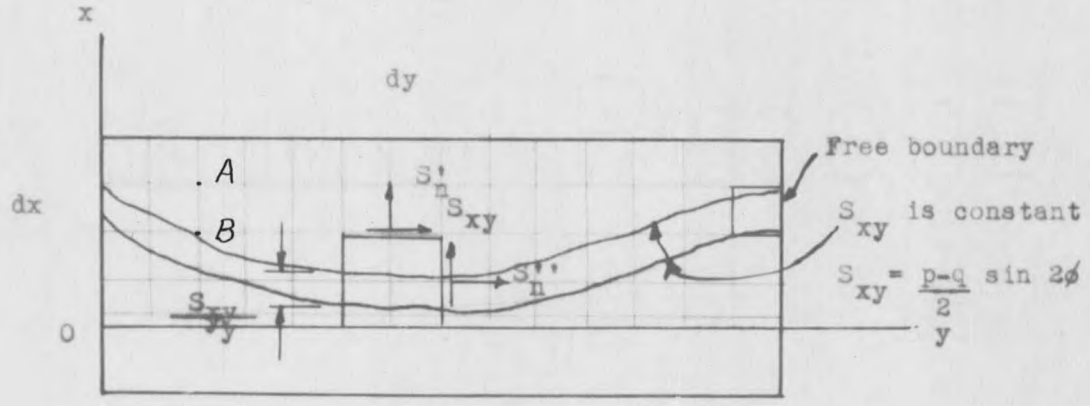


Figure C-3



Illustrating Graphical Solution to Principal Stress
* Figure C-4

* All figures suggested or duplicated from Photoelasticity by N. Alexander.

$$\left(S''_n + \frac{\partial S''_n}{\partial y}\,dy\right)dx - S''_n dx + \left(S_{xy} + \frac{\partial S_{xy}}{\partial x}\,dx\right)dy - S_{xy}dy = 0$$

which reduces to:

$$\frac{\partial S''_n}{\partial y} + \frac{\partial S_{xy}}{\partial x} = 0 \qquad (C\text{-}2)$$

Integrating between the limits 0 to x:

$$S'_{nx} = S'_{no} - \int_0^x \frac{\partial S_{xy}}{\partial y}\,dx \qquad (C\text{-}3)$$

$$S''_{ny} = S''_{no} - \int_0^y \frac{\partial S_{xy}}{\partial x}\,dy \qquad (C\text{-}4)$$

S''_{ny} = the normal stress at any point between the limits 0 to y parallel to the y axis.

S''_{no} = the known normal stress at some point in the model and it is parallel to the y axis.

$\int_0^y \frac{\partial S_{xy}}{\partial x}\,dy$ = the summation in the y direction of the variation in the shearing stress in the x direction.

Terms in equation C-3 have equivalent meanings. S'_{nx} and S'_{no} are stresses which may be found at a free boundary where one of the principal stresses and the shearing stress disappear.

The integral will be solved graphically:[24]

$$\frac{\partial S_{xy}}{\partial x} = \frac{(S_{xy})_A - (S_{xy})_B}{\Delta x}\text{, approximately}$$

S_{xyA} and S_{xyB} are shears that exist at two points a small distance Δ x apart. (See Fig. C-4). A line joining the two points is parallel to the x axis. To make a summation of the differences in shears, the shearing stress is found for several points on lines through points A and B both

24. Frocht, M. M. 1941 op. cit., p. 263.

parallel to the y axis.

For corresponding points on the lines $\frac{\Delta S_{xy}}{\Delta y}$ may be computed. Knowing these values the following step may be made:

$$\int_0^y \frac{\partial S_{xy}}{\partial x} dy = \sum_0^y \frac{\Delta S_{xy}}{\Delta x} \Delta y \text{ (approx.)} \qquad \text{(C-5)}$$

The principal stresses are found by (See Appendix B):

$$p = \frac{S_n' + S_n''}{2} \pm \sqrt{(S_{xy})^2 + \frac{(S_n' - S_n'')^2}{4}} \qquad \text{(B-19\&20)}$$

LITERATURE CITED AND CONSULTED

Alexander, N. 1936 PHOTOELASTICITY, Rhode Island State College.

Coker, E. G. and Filon, L. N. 1930 TREATISE ON PHOTOELASTICITY, Cambridge Press, London.

Frocht, Max Mark 1941 PHOTOELASTICITY, Vol. 1, John Wiley and Sons, Inc., New York.

Frocht, Max Mark 1946 PHOTOELASTICITY, Vol. 2, John Wiley and Sons, Inc., New York.

Grinter, L. E. 1947 THEORY OF MODERN STEEL STRUCTURES, Vol. 2, The MacMillan Company, New York.

Laurson, P. G. and Cox, W. J. 1947 MECHANICS OF MATERIALS, John Wiley and Sons, New York.

Riggs, Norman C. and Frocht, Max M. 1938 STRENGTH OF MATERIALS, The Ronald Press Company, New York.

Robertson, John Kellock 1935 INTRODUCTION TO PHYSICAL OPTICS, D. Van-Nostrand Company, Inc., New York.

THE POLARIZING INSTRUMENT COMPANY, 630 Fifth Avenue, New York City, New York.

MONTANA STATE UNIVERSITY LIBRARIES
3 1762 10013154 7

N378
B944d
cop.2
93821
Burroughs, M. A.
The development and use of photoelastic laboratory for Mont. St. College

DATE	ISSUED TO
APR 20 '51	Wallace Amos 311 N. Fla
JUL 6 '51	A. A. Wallace Co
JUL 28 '51	M. A. Burroughs Project
AUG 1 '51	Engr
	Fla
NOV 30 '54	
JUL 2 '60	

N378
B944d
cop.2

93821